MEMO 4-27-59E

NASA MEMO 4-27-59E

NASA

MEMORANDUM

HEAT TRANSFER FROM CYLINDERS IN TRANSITION FROM SLIP FLOW TO FREE-MOLECULE FLOW

By Ronald J. Cybulski and Lionel V. Baldwin

Lewis Research Center
Cleveland, Ohio

NATIONAL AERONAUTICS AND SPACE ADMINISTRATION

WASHINGTON

May 1959

NATIONAL AERONAUTICS AND SPACE ADMINISTRATION

MEMORANDUM 4-27-59E

HEAT TRANSFER FROM CYLINDERS IN TRANSITION FROM SLIP FLOW TO FREE-MOLECULE FLOW

By Ronald J. Cybulski and Lionel V. Baldwin

SUMMARY

Over 600 measured heat-transfer coefficients in the transition from slip to free-molecule flow have been correlated by using the Nusselt number Nu as a function of the Knudsen Kn and Reynolds Re (or Mach M) numbers. The experimental range for these heat-transfer data from transverse cylinders in air corresponds to the following dimensionless groups: M, 0.10 to 0.90; Re, 0.03 to 11.5; Kn, 0.10 to 5.0. The total air temperature T_t was maintained constant at 80° F, but wire temperature was varied from 150° to 580° F. At Kn = 0.10, Nu extrapolates smoothly into slip-flow empirical curves that show Nu as a function of Re and M or Kn. The correlation gradually changes from the $\sqrt{Re_t}$ dependence characteristic of continuum flow to first-power Re dependence as Kn increases (decreasing Re). At the experimental limit Kn ≈ 5.0, the Nu data correlate with a mean fractional error of ±13 percent by the prediction of free-molecule-flow theory. In comparing experimental results with theory, an accommodation coefficient of 0.57±0.07 was inferred from the heat-transfer data, which were obtained with etched tungsten wire in air.

The wire recovery temperature T_e was measured and compared with existing data and theory in terms of a ratio η ($\equiv T_e/T_t$). The results can be divided into three groups by Kn criteria: For Kn < 2.0, η is independent of Kn, and η decreases from 1.0 to 0.97 as M increases from 0 to 0.90; for 2.0 < Kn < 5.0, η is a function of both Kn and M in this transition region to fully developed free-molecule flow; and for Kn > 5.0, η predicted by free-molecule-flow theory is observed and η increases from 1.0 to 1.08 as M increases from 0 to 0.90, again independent of Kn. Therefore, these T_e data provide a guide to the boundary of fully developed free-molecule flow, which is inferred from this research to exist for Kn > 5.0. This boundary criterion is substantiated by other published data on T_e at supersonic speeds.

The application of fine hot wires to pressure measurement in subsonic rarefied flows is discussed. It should be possible to develop this Pirani-type gage for air pressures below 1900 microns of mercury.

INTRODUCTION

Interest in heat transfer to rarefied gas flows has grown with the advent of high-altitude satellites and missiles. The fundamental heat-transfer data presented in this report were obtained with transverse cylinders in subsonic airflows. The importance of this experimental work to problems of high-speed flight is that these heat-transfer data were obtained in the transition from slip to free-molecule flow. No theoretical approach has been successful in this transition region (ref. 1); and, as will be discussed shortly, experimental results in this flow regime are meager.

Another possible application of this research is for the development of instrumentation for low-density facilities. The conventional hot-wire anemometer, which has been a valuable tool for studying turbulent velocity fluctuations in aerodynamic research, may be valuable in low-density flow studies as a pressure gage. This application is discussed in the text.

Experimental Range of This Research

The usual dimensionless parameters used to express the gas-flow regime are the Mach number and the Reynolds number. Figure 1 is a convenient summary of recent heat-transfer experiments with transverse cylinders as the heat-transfer element. The Mach number is based on free-stream velocity and static temperatures; the Reynolds number is based on the cylinder diameter and on free-stream velocity, density, and viscosity. The shaded areas represent the work of previous investigators in the rarefied-gas regions, and these areas are keyed by numbers to the reference list of this report (refs. 2 to 16). A recent review of the previous work is given in reference 2.

Another dimensionless group, the Knudsen number Kn, is useful in rarefied-gas flows. The kinetic theory of gases relates the Knudsen number (ratio of mean free path of gas to cylinder diameter) to the ratio of Mach number to Reynolds number. For air,

$$Kn \equiv \frac{\lambda}{D_w} = 1.46 \frac{M}{Re_t} \sqrt{\frac{T}{T_t}} \tag{1}$$

(All symbols are defined in appendix A.)

The constant Knudsen number lines in figure 1 provide an approximate guide to the three broad divisions of airflow. Although these regions are probably not sharply defined, reference 14 proposes the following boundaries for flow over transverse cylinders:

(1) Continuum flow: $Kn < 0.001$

(2) Slip flow: $0.001 < Kn < 2.0$

(3) Free-molecule flow: $Kn > 2.0$

More recently, recovery-temperature data from cylinders in the low-density supersonic tunnel at the University of California (refs. 16 and 17) have indicated that fully developed free-molecule flow may not be attained until a Knudsen number of about 5.

The experimental range of the research reported here is also shown in figure 1. The boundaries shown are for Knudsen numbers from 0.10 to 5.0, Reynolds numbers from 0.03 to 11.50, and Mach numbers from 0.10 to 0.90.

Objectives of This Research

The primary objective of this work is to present an empirical Nusselt number correlation of heat-transfer data obtained in the transition from slip to free-molecule flow. The need for an experimental approach in this region has already been mentioned. At the lower Reynolds number limit of this research where fully developed free-molecule flow is approached, it will be possible to compare predictions of the theory for very rarefied-gas flow with experimental observations. No verification of free-molecule-flow analysis for heat transfer has been published for subsonic and transonic flows; verification to date has been limited to supersonic streams (refs. 14 and 16). That this research will fill an existing gap in the literature can be seen readily in figure 1.

Another main objective of this research is to obtain data on the equilibrium or recovery temperature of a cylinder in the transition to free-molecule flow. No data in subsonic flows have been reported previously. These measurements serve as a direct test (independent of empirical constants) for the boundary of the free-molecule-flow regime.

Specification of the Knudsen number above which the theory of very rarefied-gas flow applies is also an objective.

Finally, an attempt will be made to infer an accommodation coefficient for tungsten wire in air from the heat-transfer data. The significance of this empirical constant is discussed in the text.

APPARATUS AND PROCEDURE

The equipment and procedure used in this research are similar to those described in reference 2. Therefore, this section will present only an outline, particularly pointing out significant departure from the methods of the previous report.

Apparatus

Tunnel and air facility. - A sketch of the variable-density, low-turbulence tunnel is shown in figure 2. Dry air at ambient temperature passed through the cone-shaped filter before entering the $1\frac{1}{2}$-inch-diameter test section. The insert in figure 2 shows a detail of the packing gland, which provided a vacuum seal around the probe but allowed the probe to be moved out of the tunnel for airflow adjustments.

The air velocity in the test section was calculated from the mass-flow rate, which was metered by a calibrated sonic orifice upstream of the filter. Two orifices of different capacity were used in the course of the experiment.

The tunnel was serviced by the central air facilities at the Lewis Research Center. The exhaust pressure is normally 4.0 inches of mercury absolute, but this was extended to 0.05 inch absolute by two stream ejectors in series downstream of the test section. The static pressure in the test section could be varied from 0.05 to 4.0 inches of mercury. A dibutylphthalate U-tube manometer was used to measure the static pressure in the test section by referencing one arm of the U to a 50-micron reservoir. The pressure upstream of the sonic orifice was read from calibrated mercury manometers.

The total air temperature was $80^{\circ}\pm5^{\circ}$ F, and it was measured with a calibrated thermocuople located in the inlet of the nozzle (fig. 2).

Probe design and tungsten wire. - A sketch of the probe used in this investigation is shown in figure 3. Since the length of the wire was about 2500 times its diameter, flow interference of the probe prongs was minimized. Early in this investigation, it was found that air leaked through some of the probe bodies. Careful cementing of internal probe parts was necessary to make the probe design used herein suitable for vacuum applications.

Tungsten wire was the heat-transfer element of the probe. The wire had a nominal diameter of 0.00020±0.00002 inch. A diameter as determined from electron photomicrographs in reference 2 was 2.2×10^{-4} inch. However, the diameter from the spool section used in this work was calculated from electrical resistance measurements to be intermediate between the nominal diameter and that used in reference 2. A diameter of 2.11×10^{-4} inch was used for the calculations in this report.

One of the most important physical properties of tungsten in the calculations of heat-loss data is the relation between electrical resistance and temperature. Seven wire samples were silver-soldered to probes, annealed, and then placed in a small calibration heater (fig. 4). At various air temperatures in the heater, the wire resistance was determined by balancing a Kelvin double bridge while passing a small detection current (which did not heat the wire within the sensitivity of measurement) through the wire. A sample calibration curve is given in figure 5. A least-square solution for the best parabola $\left\{\Omega = \Omega_0\left[1 + \alpha_w(T - 32) + \beta_w(T - 32)^2\right]\right\}$ through the calibration points yielded the coefficients shown in figure 5. In this manner, the average second-order coefficient β_w was found to be 2.67×10^{-7} $^{\circ}F^{-2}$. For all wires subsequently used in the tunnel, only a partial calibration from 32° to 200° F was determined. Then assuming a value of $\beta_w = 2.67\times10^{-7}$ $^{\circ}F^{-2}$, a least-square solution for Ω_0 and α_w was calculated for each wire used. Table I summarizes the physical constants of the wire samples used in the heat-loss measurements.

Anemometer electrical equipment. - The fine-wire probe formed one arm of a Kelvin double bridge. The bridge described in reference 9 was used; the only modification was to change the standard resistor to 100 ohms. The electrical power into the bridge for hot-wire operation was controlled by the constant-average-temperature servo described in reference 2. The desired hot-wire resistance was set on the bridge, and the power necessary to heat the wire to this resistance was calculated from the voltage drop measured across the hot wire by a potentiometer.

The recovery resistance was measured by balancing the bridge when a negligible detection current was flowing through the wire. The use of the Kelvin double bridge made it possible to determine the wire resistance while almost completely eliminating lead resistances from the measurements.

Procedure

The tunnel was operated at various Mach numbers from 0.10 to 0.90. The range of Knudsen number based on wire diameter was 0.10 to 5.0, which corresponds to static air densities from about 0.0090 to 0.0002 pound (mass) per cubic foot. An important feature of the procedure was a rather random schedule for taking data, as can be seen in table II from the chronological run numbers. This reduced the probability of systematic error in the measurements.

After tunnel conditions had been adjusted, the probe was moved into the test section, and manometer readings and temperature were recorded. The recovery resistance was measured, after which six progressively higher hot-wire resistances were set on the bridge, and the power input to the wire was determined for each setting. Then the recovery temperature was again recorded along with tunnel operating conditions.

DIMENSIONLESS GROUPS OF CORRELATION

This section is devoted to a brief explanation of the dimensionless parameters used in correlating the data.

The convective heat-loss rate defines the heat-transfer coefficient h:

$$Q_C = h\pi D_w l(T_w - T_e) \tag{2}$$

The heat-transfer coefficient is defined in terms of the recovery temperature T_e; thus, for the adiabatic wire, $T_w = T_e$.

The Nusselt number is defined as

$$Nu_t = \frac{hD_w}{k_t} = \psi \frac{J'V_w^2}{\pi l k_t \Omega_w (T_w - T_e)} \tag{3}$$

The air thermal conductivity k_t is evaluated at total air temperature using the values given in reference 18. Two published correction procedures were used to account for the heat loss by conduction from the hot wire to the supports. Each procedure gave a correction factor ψ; and, as discussed in reference 2, this factor was nearly identical in numerical value for both end-loss computations. Radiant heat loss from the wire was calculated to be negligible for all operating conditions.

The wire temperature for both hot-wire operation and recovery-temperature measurements was calculated from the resistance-temperature calibration:

$$\Omega = \Omega_0\left[1 + \alpha_w(T - 32) + \beta_w(T - 32)^2\right] \tag{4}$$

The Reynolds number for the wire was defined by the wire diameter and the free-stream (or static) density and velocity. The air viscosity μ_t was evaluated at total air temperature using values given in reference 18:

$$Re_t = \frac{\rho U D_w}{\mu_t} \tag{5}$$

The Knudsen number was calculated from free-stream density and the wire diameter using the formula suggested by reference 13:

$$Kn = \frac{\lambda}{D_w} = \frac{1.5870\ 10^{-8}}{\rho D_w} \tag{6}$$

The constant 1.5870×10^{-8} has the units (lb mass)/(sq ft). Equation (6) assumes that the mean free path for air λ is given by elementary kinetic theory and that $\rho\lambda$ is a constant.

The Mach number was calculated from the velocity measured with a sonic orifice and the static temperature:

$$M = \frac{U}{49.02\sqrt{T}} \tag{7}$$

The data reduction of this research was performed on the IBM 653 digital computer.

RESULTS AND DISCUSSION

The presentation and discussion of results is divided into three parts. In the first section, the recovery-temperature results are presented and are compared with other available recovery temperature data and theoretical predictions of recovery temperature. In the second section, the heat-transfer results are given under the heading "Nusselt Number Correlation." Finally, the application of this research to low-density flow instrumentation is examined.

Recovery Temperature

A survey of published data on recovery temperature of transverse cylinders in subsonic airflows is summarized in figure 6. Each curve is keyed to the reference source. These data were obtained over a wide Reynolds number range. Reference 12 data extended to $Re_t \approx 30,000$ or $Kn \approx 4\times10^{-5}$, which is well into continuum flow. The data from reference 13 were obtained in slip flows to a limiting Knudsen number of 0.10. Previous investigations (e.g., refs. 12 and 13) indicate that the recovery temperature is a function only of Mach number and is nearly independent of Knudsen number within experimental scatter for at least $4\times10^{-5} < Kn < 0.10$.

However, both theory (ref. 14) and previous experiments (refs. 14, 16, 17, and 19) have shown that the temperature of a transverse cylinder will exceed the total temperature of the gas stream in which it is located when the cylinder is placed with its axis perpendicular to a uniform gas stream in which the mean free path is several times greater than the cylinder diameter. This temperature is a function only of the Mach number, static air temperature, and the number of excited degrees of freedom of the gas molecules. The equation for the recovery temperature of an infinite cylinder $T_{e,\infty}$ placed in a diatomic gas flow is given in references 14 and 19 as

$$\frac{T_{e,\infty}}{T_t} = \frac{T}{T_t}\,\frac{f(s)}{g(s)} \tag{8}$$

where $f(s)$ and $g(s)$ are dimensionless functions of the molecular speed ratios s. The molecular speed ratio is related to the more familiar Mach number as follows:

$$s = \sqrt{\frac{\gamma}{2}}\,M \tag{9}$$

For convenience, the functions $f(s)$ and $g(s)$ are tabulated over the range of interest in this report in table III.

Equation (8) is plotted in figure 7. It is important to notice that for free-molecule flow the theory predicts that the recovery-temperature ratio η is a function only of Mach number. However, as was pointed out in the INTRODUCTION, the boundary for fully developed free-molecule flow is uncertain.

The recovery-temperature results of this research were obtained with a finite length of wire. An equation (B9) is derived in appendix B to account for conduction heat loss from a wire to its supports. The maximum departure from infinite wire behavior for the 0.50-inch tungsten wires used for this research was calculated to be 2 percent. Therefore, no correction has been applied to the measured recovery-temperature data, which will be assumed to be obtained from infinite wires. This statement does not apply to hot-wire operation in the determination of Nusselt number.

The results obtained in this research are given in table IV and are shown in figure 8, in which the ratio of recovery temperature to total temperature is compared with the curves from continuum- and slip-flow experiments (fig. 6) and free-molecule-flow theory (fig. 7). The data on the recovery-temperature ratio η can be divided into three regions: The first is for $Kn < 2.0$, where η is only Mach number dependent and decreases from 1.0 to 0.97 as Mach number increases from 0 to 0.90; a transition region is then discernible in which η is a function of both Mach and Knudsen numbers, and the constant Kn lines begin to approach the predicted theoretical curve for fully developed free-molecule flow; finally, for Kn greater than about 5.0, η is again independent of Kn and increases from 1.0 to 1.08 as Mach number increases from 0 to 0.90.

Figure 9 shows a comparison of the measured recovery temperature T_e of figure 8 and the theoretical recovery temperature $T_{e,\infty}$ in free-molecule flow. The ratio of T_e to $T_{e,\infty}$ is shown here as a function of Knudsen number. The value of Knudsen number where $T_e/T_{e,\infty}$ is equal to unity is a criterion for the attainment of fully developed free-molecule flow. This value appears to be about $Kn = 5.0$ in figure 9. It is important to recall that this result is independent of empirical constants (i.e., accommodation coefficient), as can be seen in equation (8). Approximately the same value of Knudsen number ($Kn = 5.0$) for fully developed free-molecule flow was obtained in the work of references 16 and 17, although these studies were carried out for supersonic flows. The inference that the boundary for free-molecule flow may be taken as $Kn > 5.0$ appears to be contrary to the conclusions from the pioneer work of reference 19. Reference 19 proposed that the boundary criterion was $Kn > 2.0$. A close look at the data of reference 19 shows that lack of sufficient data in the range $1.0 < Kn < 5.0$ could easily account for the difference in the proposed criterion. Finally, it should be pointed out that the dashed lines of constant Mach number for $0.10 < Kn < 1.0$ in figure 9 connect the present data with values calculated from the reference 9 curve in figure 6.

Nusselt Number Correlation

Before presenting the heat-transfer results of this investigation, it will be convenient to outline the form that the Nusselt number correlation should be expected to take in the transition from slip to free-molecule flow. Figure 10 (from ref. 2) is an attempted Nusselt number correlation in subsonic continuum, slip, and free-molecule flow. In figure 10, the Nusselt number is shown as a function of Reynolds number; constant Mach number and Knudsen number parametric curves are shown solid and dashed, respectively.

For Reynolds numbers between 250 and 30,000, the empirical correlation given in reference 12 is plotted. The important feature of this relation for cylinders in continuum flow is that the Nusselt number is well correlated by $\sqrt{Re_t}$. Note that changing the subsonic Mach number has small percentage effect on Nu_t at constant Re_t.

The correlation shown for $1.0 < Re_t < 100$ in figure 10 is based on the slip-flow data from reference 2. The increasing necessity for an additional parameter other than the Reynolds number to correlate the experimental heat-transfer data shows clearly in this slip-flow region as Re_t decreases. This additional parameter is either the Mach number or the Knudsen number. Both forms that this correlation might take are shown in figure 10; that is, $Nu_t = f(Re_t,M)$ and $Nu_t = f(Re_t,Kn)$ are both given. However, only one additional parameter (M or Kn) is independent, since these groups are related by equation (1). Since the need for the additional parameter is the result of the slip or rarefied-gas phenomenon, it seems preferable to view the Knudsen number as the additional independent parameter.

The Nusselt number correlation shown in figure 10 for $Re < 1.0$ is a prediction of free-molecule-flow theory (using an accommodation coefficient $\alpha = 0.90$), which will be discussed in detail later. Note that the theory predicts first-power Reynolds number dependence and a large separation of the constant M parametric curves. Furthermore, it is clear that, although the slip-flow data extrapolate smoothly into the continuum curves in the region $Re_t \approx 100$, the free-molecule-flow prediction does not agree quantitatively with the slip-flow data around $Re_t \approx 1.0$. With this discussion as a background, the results of this research will now be examined.

A representative portion of the heat-transfer data obtained in this experiment is shown in figure 11. These data were obtained at a total air temperature of 80° F and a cylinder temperature of 580° F. Both forms of the Nusselt number correlation are shown in figure 11; that is, $Nu_t = f(Re_t,Kn)$ and $Nu_t = f(Re_t,M)$. It will be convenient to discuss figure 11 from two points of view: first, to compare the correlation at $Kn = 0.109$ with the slip-flow results presented in figure 10; then, to compare the data at $Kn = 4.70$ with free-molecule-flow theory. The general lack of scatter in the data, as shown in figure 11 for $0.109 < Kn < 4.70$, makes it unnecessary to discuss the internal consistency of the data between the experimental limits.

Figure 12 compares the lower Knudsen number portion of the data from this report with the slip-flow data from reference 2. The two sets of data agree quite well, and the same trends noted in reference 2 are present here. These are (1) a gradual change in slope of the constant Mach number parametric lines from fractional-power to first-power Reynolds number dependence as Re decreases; (2) a large separation of the constant Mach number curves, showing decreasing dependence of heat transfer on air velocity, especially in low subsonic flows; and (3) the increasing importance of the Knudsen number as the governing parameter for subsonic flows as Re decreases.

Before comparing the high Knudsen number data with free-molecule-flow predictions, it is convenient to review the results of the free-molecule-flow analysis for heat transfer from cylinders, which is given in detail by references 14 and 19. Reference 19 gives the following equation for the heat-transfer coefficient h:

$$h = \frac{p v_m \alpha [g(s)]}{2J(\pi^{3/2})T} \tag{10}$$

Reexpressing equation (10) in the more conventional terms of Nusselt number shows that

$$Nu_t = \left[\left(\frac{R\mu_t}{2J\pi k_t}\right)\alpha\right] \frac{g(s)}{Kn} \sqrt{\frac{T}{T_t}} \tag{11}$$

The accommodation coefficient α is a way of expressing the efficiency of the energy-exchange process that occurs between a solid surface and an impinging molecular stream (ref. 20). The definition can be written as follows:

$$\alpha = \frac{E_i - E_r}{E_i - E_w} \tag{12}$$

At present, the accommodation coefficient can be considered an empirical constant that depends not only on the metal and its surface finish but also on the gas. Generalizations concerning the accommodation coefficient are scant and not without exception. Therefore, α can be regarded as an undetermined constant when equation (11) is evaluated for a total air temperature of 80° F.

The following equation predicts Nu_t as a function of the Knudsen and Mach numbers where the free-molecule-flow theory applies (i.e., $Kn > 5.0$) and the accommodation coefficient is known:

$$Nu_t = 0.03214(\alpha) \frac{g(s)}{Kn} \sqrt{\frac{T}{T_t}} \tag{13}$$

In order to estimate the accommodation coefficient of the tungsten wire in air, it was necessary to assume that equation (13) is valid for Kn = 4.00 and 4.70, which are the limits of the experimental data. Table V summarizes the results of solving equation (13) for α using the Nusselt number measurements of this experiment. An accommodation coefficient of 0.57 ± 0.07 for tungsten wire in air was determined in this manner.

It is now possible to compare the high Knudsen number portion of the heat-transfer data with free-molecule-flow predictions. Figure 13 shows this comparison. In evaluating the theoretical curves from equation (13), an accommodation coefficient of 0.57 has been used for all flow conditions. From figure 13, the agreement between theory and experiment can be seen to be adequate for most engineering purposes. More specifically, equation (13) and $\alpha = 0.57$ predicted the observed Nusselt numbers at Kn = 4.00 and 4.70 with an average deviation of a single observation of ± 0.00537, which corresponds to a mean percentage error in Nusselt number of about ± 13 percent.

Equation (13) suggests another method of presenting heat-transfer data in free-molecule flow. Figure 14 is a plot of equation (13) with $\alpha = 0.57$. This figure will be referred to in the next section.

Only a portion of the data given in table II are shown in figure 11. The remainder of the data were obtained at wire temperatures lower than 580° F but at the same flow conditions. This discussion of the results at lower wire temperatures has been deferred until now because these data generally only verify the results at $T_W = 580^{\circ}$ F. A series of plots substantiating this statement is given in figure 15. The general appearance of figure 15 at $T_W = 580^{\circ}$ F is repeated in all six parts at the lower wire temperatures. The data scatter increases with decreasing wire temperature; but it is clear that, if the wire temperature affects the measured Nusselt numbers, it is a secondary effect.

Application to Low-Density Instrumentation

Fine wires have been used as hot-wire anemometers to measure time-mean and turbulent fluctuating air velocities for many years. During the majority of this time, it was not recognized that the flow over the sensitive element was a rarefied-gas flow. That is, even though the air was at atmospheric density, the fine wire was in slip flow. Thus, hot-wire calibrations based on King's equation (e.g., see ref. 21) are somewhat in error, and this fact has been discussed in recent reports (refs. 2 and 13). On the other hand, fine hot wires are the sensitive element of pressure-measuring gages that were developed before the advent of the anemometer in 1914. The Pirani or thermal-conductivity gages are hot wires whose heat loss is calibrated in pressure units, usually in the range 10 to 200 microns of mercury. Since both anemometer and Pirani gage applications depend on the heat-loss characteristics of fine wires, it is appropriate to relate the data of this research to these instruments.

The convective heat loss from cylinders over a wide range of airflow conditions may be predicted by using figure 16. For flow of air at ambient temperature and pressure, the Knudsen number for a 0.00020-inch-diameter wire is about 0.012. Therefore, the measured convective heat-loss rate (i.e., Nu_t) may be used in principle to infer an air velocity (from either M or Re) by using figure 16. In practice, an instrument calibration, which is obtained within the restrictive limits of application, is substituted for figure 16. However, it is not anemometer applications that are to be discussed here. The purpose of this discussion is to point out the gradual change in heat-loss characteristics that makes the fine hot wire applicable to pressure measurements as the flow over the wire changes from slip to free-molecule flow. This transition to very rarefied airflow causes the change in heat-transfer-coefficient calibration shown in figure 16 as Knudsen number increases from about 0.012 to 5.0. The velocity sensitivity of the wire decreases monatomically as the Knudsen number increases; and, when the flow over the wire becomes a fully developed free-molecule flow, the velocity sensitivity has all but vanished in the subsonic regime. This point is best observed in figure 14. Note that, at any constant air density (i.e., constant $1/Kn$, fig. 14), the percentage change in heat-transfer rate, as given by Nu_t, is very small due to changes in airflow rate from stagnant air ($M = 0$) to about $M = 0.4$. More specifically, using equation (13) and the tabulated values of $g(s)$ in table III, the heat-transfer rate is calculated to increase only about 5 percent as M varies from 0 to 0.40. Recalling that equation (13) can be applied for all $Kn > 5.0$ according to this research, then it is apparent that a 0.00020-inch-diameter hot wire could be used as an air pressure gage for flowing air at room temperature below about 1900 microns of mercury. This instrument would require less than a 5-percent air velocity correction for $U < 400$ feet per second; the corrections for heat conduction to wire supports and radiation to surroundings are usually greater than 5 percent for Pirani gages (e.g., see ref. 22).

In the previous paragraph, a possible extension of Pirani-type gages to pressure measurements with the sensitive element placed in subsonic airflows has been suggested. Naturally, the principle would apply equally well to any gas in a free-molecule flow if the appropriate manatomic or diatomic gas equation is used (ref. 19). Finally, the application of equation (13) to instrumentation in supersonic free-molecule flows has been the subject of several University of California (Berkeley) reports (refs. 16, 17, and 23). It is interesting to note that, for Mach numbers greater than about 2, the hot-wire sensitivity is governed by the first power of the Reynolds number almost independent of Mach number. Thus, for $M > 2.0$, the fine wire is almost equally sensitive to air density and to velocity in a free-molecule flow.

CONCLUDING REMARKS

The following conclusions can be drawn from the heat-transfer measurements reported herein in the transition region from slip to free-molecule flow:

1. The Nusselt number Nu_t correlation for transverse cylinders in subsonic airstreams is complicated in the transition regime from slip flow to free-molecule flow. No simple-power-law engineering equation has been found for this Nusselt number correlation, but it is conveniently given in graphical form (fig. 11). Figure 11 shows Nu_t as a function of Reynolds number Re_t with constant Mach number M and Knudsen number Kn parametric lines. The three important features of this correlation are:

(a) The gradual change in slope of the constant M parametric lines from fractional-power to first-power Reynolds number dependence as Re_t decreases

(b) Large separation of the constant M curves showing decreasing dependence of heat transfer on air velocity

(c) The increasing importance of Kn as the governing parameter for subsonic flows as Re_t decreases.

2. The measured Nusselt numbers of this report are compared with published slip-flow data at $Kn = 0.077$ and free-molecule theory at $Kn > 5.0$ in figures 12 and 13, respectively. The agreement at low Kn with slip-flow data is good; and, by assuming an accommodation coefficient α of 0.57, the data agree adequately with predictions of free-molecule-flow theory. That is, for $Kn > 4.0$, the data are correlated with an average deviation of ±13 percent by

$$Nu_t = 0.03214\ (\alpha)\ \frac{g(s)}{Kn} \sqrt{\frac{T}{T_t}}$$

where $g(s)$ is a Mach number function defined by theory, T is static temperature, and T_t is total air temperature.

3. An average accommodation coefficient α of 0.57±0.07 can be inferred from the measured heat-transfer coefficients of etched tungsten wire in subsonic airflows.

4. The transition to fully developed free-molecule flow appears to be complete at $Kn = 5.0$ for transverse cylinders in subsonic flow. This conclusion is based on the comparison of measured recovery temperature with theoretically predicted recovery temperature as shown in figure 9. The inference does not depend on empirical constants; that is, it is independent of accommodation coefficient.

5. The recovery-temperature data of this report can be divided into three regimes by Knudsen number criteria, as can be seen in figure 8: $Kn < 2.0$, the ratio of recovery to total air temperature $\eta \equiv (T_e/T_t)$ is independent of Kn and η decreases from 1.0 to 0.97 as Mach number increases from 0 to 0.90; $2.0 < Kn < 5.0$, η is a function of both Kn and M in this transition region to fully developed free-molecule flow; $Kn > 5.0$, η predicted by free-molecule flow theory is observed and η increases from 1.0 to 1.08 as M increases from 0 to 0.90, again independent of Kn.

Lewis Research Center
National Aeronautics and Space Administration
Cleveland, Ohio, January 30, 1959

APPENDIX A

SYMBOLS

A_w cross-sectional area of cylinder, $\pi D_w^2/4$, sq ft

Bi Biot number, hD_w/K_w, dimensionless

D_w wire diameter, ft or in.

E_i rate of incident molecular energy

E_r rate of reemitted molecular energy

E_w rate of reemitted molecular energy that would be carried by the scattered stream if it were a stream issuing from a gas in equilibrium at the surface temperature T_w

$f(s)$ dimensionless function of s; $f(s) = \pi\left[\exp\left(-\frac{s^2}{2}\right)\right]$

$$\times\left\{(s^2 + 3)I_0\left(\frac{s^2}{2}\right) + \left(s^2 + \frac{7}{2}\right)s^2\left[I_0\left(\frac{s^2}{2}\right) + I_1\left(\frac{s^2}{2}\right)\right]\right\}$$

$g(s)$ dimensionless function of s; $g(s) = 3\pi\left[\exp\left(-\frac{s^2}{2}\right)\right]$

$$\times\left[(1 + s^2)I_0\left(\frac{s^2}{2}\right) + s^2 I_1\left(\frac{s^2}{2}\right)\right]$$

g_c unit conversion factor, $(\mathrm{lb(M)})(\mathrm{ft})/(\mathrm{lb(F)})(\mathrm{sec}^2)$

h convective heat-transfer coefficient, Btu/(sec)(sq ft)($^{\circ}$F)

$I_0(z)$, $I_1(z)$ modified Bessel function of first kind, zero and first order, respectively, dimensionless

J conversion factor, ft-lb(F)/Btu

J' conversion of watts to Btu/sec, 9.484×10^{-4}

K_w thermal conductivity of cylinder metal, Btu/(sec)(ft)($^{\circ}$F)

Kn Knudsen number, λ/D_w

k_t thermal conductivity at total air temperature, Btu/(sec)(ft)($^{\circ}$F)

l length of wire, ft

M	Mach number
m	mass of 1 molecule, lb(M)/molecule
Nu_t	Nusselt number, hD_w/k_t
Nu_t''	Nusselt number uncorrected for heat loss to supports
n,n'	number of molecules striking body, molecules/(sq ft)(sec)
p	static pressure, lb(F)/sq ft
Q	length-average heat-loss rate, Btu/sec
R	gas constant for air, ft-lb(F)/(lb(M))($^{\circ}$F)
Re_t	Reynolds number, $\rho D_w U/\mu_t$
r	wire radius, ft
s	molecular speed ratio, $\sqrt{\gamma/2}\ M$
T	static or free-stream air temperature, $^{\circ}$R
T_e	recovery or equilibrium wire temperature, $^{\circ}$R
$T_{e,\infty}$	theoretical recovery temperature of infinitely long cylinder in free-molecule flow, $^{\circ}$R
T_e^*	theoretical recovery temperature of finite-length cylinder in free-molecule flow, $^{\circ}$R
T_t	total air temperature, $^{\circ}$R
T_w	length-average wire temperature, $^{\circ}$F
t_w	local wire temperature at any point x, $^{\circ}$F
U	free-stream air velocity, ft/sec
V_w	wire potential, volts
v_m	most probable molecular speed, $\sqrt{2g_c RT}$, ft/sec
x	any position along length of wire, $x = 0$ at wire center, ft
α	accommodation coefficient (eq. (12)), dimensionless

α_w first-order coefficient of electrical resistance - temperature relation, $^{\circ}F^{-1}$

β_w second-order coefficient of electrical resistance - temperature relation, $^{\circ}F^{-2}$

γ ratio of specific heats, 1.4 for air

η recovery-temperature ratio, $\eta \equiv T_e/T_t$

$\varkappa$ Boltzmann constant, 5.66×10^{-24} ft-lb(F)/($^{\circ}$F)(molecule)

λ mean free path of air, ft

μ air viscosity, lb(M)/(ft)(sec)

ξ temperature variable defined by equation (B5)

ρ free-stream air density, lb(M)/cu ft

σ coefficient defined in equation (B3), dimensionless

σ_1 coefficient defined in equation (B3), $^{\circ}$R

ψ end-loss correction ratio, dimensionless

Ω_w length-average wire resistance at hot-wire temperature T_w, ohms

Ω_0 length-average wire resistance at 32° F, ohms

Subscripts:

av average

C convection

calc calculated

meas measured

t total air temperature T_t

APPENDIX B

ANALYSIS FOR RECOVERY TEMPERATURE OF FINITE TRANSVERSE CYLINDER IN FREE-MOLECULE FLOW FIELD

In order to compare theory with experiment accurately, it is necessary to recognize that the experimental cylinder has finite length. When the cylinder is operated as a hot wire by electrical heating, it is convenient to make a correction to the measured power input to account for the heat-loss rate to the supports. Such a procedure has been used in this report and in most previous hot-wire heat-loss reports to eliminate the aspect ratio (l/D_w) of the wire as a parameter (e.g., see ref 2). However, a different approach is useful when considering the recovery temperature of a cylinder in a free-molecule flow field. It is more convenient to account for the conduction loss to the supports in a theoretical analysis and thereby obtain the recovery temperature predicted for a given finite cylinder length. Then, the measured recovery temperature of the wire can be compared with the theoretical predictions for the particular finite cylinder. The purpose of this appendix is to develop an expression for the theoretical recovery temperature of a finite cylinder in a free-molecule flow field.

The calculation of the heat-transfer process between the cylinder and the diatomic gas has been given in detail in reference 19. Neglecting the radiant heat loss and any electrical power input, the energy balance equation on the entire finite cylinder is as follows:

$$2\int_0^{l/2} \alpha D_w \left\{\int_0^{\pi/2} n\left[\frac{mU^2}{2g_c} + (\psi + 1)\varkappa T\right] d\theta + \int_0^{\pi/2} n'\left[\frac{mU^2}{2g_c} + (\psi' + 1)\varkappa T\right] d\theta\right\} dx -$$

$$2\int_0^{l/2} 3\alpha D_w \varkappa\left(\int_0^{\pi/2} n\ d\theta + \int_0^{\pi/2} n'\ d\theta\right) t_w\ dx + 2JK_wA_w \left.\frac{dt_w}{dx}\right|_{l/2} = 0 \qquad \text{(B1)}$$

Equation (B1) corresponds with equation (13) of reference 19, but equation (B1) includes the conduction of heat to the cylinder supports. The coordinate system is

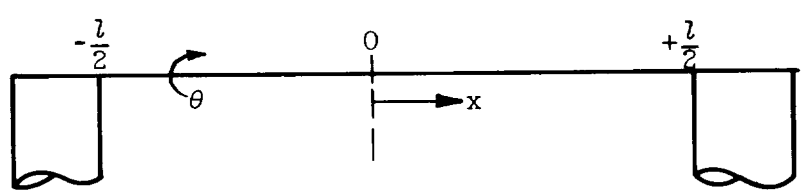

By differentiating equation (B1) with respect to x, the desired energy-balance equation is obtained as a second-order differential equation with constant coefficients:

$$\frac{d^2t_w}{dx^2} - \frac{6\alpha r\varkappa}{JK_wA_w}\left(\int_0^{\pi/2} n\ d\theta + \int_0^{\pi/2} n'\ d\theta\right)t_w$$

$$= -\frac{2\alpha r}{JK_wA_w}\left\{\int_0^{\pi/2} n\left[\frac{mU^2}{2g_c} + (\psi + 1)\varkappa T\right]d\theta + \int_0^{\pi/2} n'\left[\frac{mU^2}{2g_c} + (\psi' + 1)\varkappa T\right]d\theta\right\} \quad \text{(B2)}$$

It is convenient to introduce two symbols for the coefficients, as follows:

$$\sigma \equiv \frac{6\alpha r\varkappa}{JK_wA_w}\left(\int_0^{\pi/2} n\ d\theta + \int_0^{\pi/2} n'\ d\theta\right)$$

and

$$\sigma_1 \equiv \frac{2\alpha r}{JK_wA_w}\left\{\int_0^{\pi/2} n\left[\frac{mU^2}{2g_c} \quad (\psi + 1)\varkappa T\right]d\theta \quad \int_0^{\pi/2} n'\left[\frac{mU^2}{2g_c} \quad (\psi' + 1)\varkappa T\right]d\theta\right\} \quad \text{(B3)}$$

All the integrals in equations (B3) are evaluated in reference 19. Using these results, it is a straightforward but lengthy procedure to show that the ratio (σ_1/σ) is the solution for the recovery temperature of an infinitely long cylinder (ref. 14):

$$\frac{\sigma_1}{\sigma} \equiv T_{e,\infty} = T\,\frac{f(s)}{g(s)} \quad \text{(B4)}$$

Equation (B2) can be reduced to a homogeneous equation by the following change of variable:

$$\xi \equiv \frac{\sigma_1}{\sigma} - t_w \quad \text{(B5)}$$

With the use of equation (B5), equation (B2) becomes

$$\frac{d^2\xi}{dx^2} + \sigma\xi = 0 \quad \text{(B6)}$$

The following boundary conditions will be used to find the temperature distribution along the wire length:

(1) Since the wire is symmetrical, at the center of the wire ($x = 0$) the temperature gradient must be zero:

$$\left.\frac{dt_w}{dx}\right|_{x=0} = \left.\frac{d\xi}{dx}\right|_{x=0} = 0$$

(2) The temperature at each support ($x = \pm l/2$) is $T_{e,s}$, where $T_{e,s}$ is the recovery temperature for the wire supporting prongs. Since the supports are large compared with the fine wire, the support recovery temperature is governed by the empirical recovery-temperature ratio η for transverse cylinders in continuum and slip flow. That is,

$$T_{e,s} = \eta T_t = f(M)$$

The functional dependence on Mach number is a topic of this report (e.g., see fig. 6). In summary,

$$\left.t_w\right|_{x=\pm(l/2)} = T_{e,s} = f(M)$$

The solution of equation (B6) satisfying the boundary conditions can be written in terms of t_w as

$$t_w = T_{e,\infty} - (T_{e,\infty} - T_{e,s}) \frac{\cosh \sqrt{\sigma}\, x}{\cosh \frac{\sqrt{\sigma}\, l}{2}} \tag{B7}$$

The desired length-average recovery temperature of the finite cylinder in a free-molecule flow field is obtained by integrating over the length:

$$T_e^* = \frac{1}{l}\left[\int_{-l/2}^{l/2} T_{e,\infty}\, dx - \int_{-l/2}^{l/2} \frac{(T_{e,\infty} - T_{e,s})}{\cosh \frac{\sqrt{\sigma}\, l}{2}} \cosh \sqrt{\sigma}\, x\, dx\right] \tag{B8}$$

In final form,

$$T_e^* = T_{e,\infty} - \frac{T_{e,\infty} - T_{e,s}}{\frac{\sqrt{\sigma}\, l}{2}} \tanh \frac{\sqrt{\sigma}\, l}{2} \tag{B9}$$

Equation (B9) gives the theoretical recovery temperature T_e^* of a finite cylinder in a free-molecule flow field.

Finally, it is interesting to note the significance of the term $\sqrt{\sigma}\,l/2$ in the conduction correction term. It can be shown that this term is related to the predicted Nusselt number for an infinite cylinder in a free-molecule flow as given by reference 14. That is,

$$\frac{\sqrt{\sigma}\,l}{2} \equiv \sqrt{\frac{k_t Nu_t}{K_w}}\,\frac{l}{D_w} \tag{B10}$$

Here, $k_t Nu_t$ is the predicted heat-transfer coefficient hD_w given in the text as equation (13). The square-root term on the right side of equation (B10) occurs frequently in heat-transfer calculations; and, because it is dimensionless, this term has been called the Biot number Bi (ref. 24, appendix A),

$$\frac{\sqrt{\sigma}\,l}{2} \equiv \sqrt{Bi}\left(\frac{l}{D_w}\right) \tag{B11}$$

REFERENCES

1. Tsien, Hsue-Shen: Superaerodynamics, Mechanics of Rarefied Gases. Jour. Aero. Sci., vol. 13, no. 12, Dec. 1946, pp. 653-664.

2. Baldwin, Lionel V.: Slip-Flow Heat Transfer from Cylinders in Subsonic Airstreams. NACA TN 4369, 1958.

3. Carbon, M. W., Kutsch, H. J., and Hawkins, G. A.: The Response of Thermocouples to Rapid Gas-Temperature Changes. Trans. ASME, vol. 72, no. 5, July 1950, pp. 655-657.

4. Fiock, Ernest Franklin: Ninth Monthly Report of Progress on the Development of Thermocouple Pyrometers for Gas Turbines. NBS, Sept. 6, 1946.

5. Glawe, George E., and Johnson, Robert C.: Experimental Study of Heat Transfer to Small Cylinders in a Subsonic, High-Temperature Gas Stream. NACA TN 3934, 1957.

6. Kovásznay, Leslie S. G., and Törmarck, Sven I. A.: Heat Loss of Hot-Wires in Supersonic Flow. Bumblebee Rep. No. 127, Dept. Aero., The Johns Hopkins Univ., Apr. 1950. (Contract NOrd 8036 with Bur. Ord.)

7. Laufer, J., and McCellan, R.: Measurement of Heat Transfer from Fine Wires in Supersonic Flows. Jour. Fluid Mech., vol. 1, pt. 3, Sept. 1956, pp. 276-289.

8. Laurence, James C., and Landes, L. Gene: Auxiliary Equipment and Techniques for Adapting the Constant-Temperature Hot-Wire Anemometer to Specific Problems in Air-Flow Measurements. NACA TN 2843, 1952.

9. Lowell, Herman H.: Design and Applications of Hot-Wire Anemometers for Steady-State Measurements at Transonic and Supersonic Airspeeds. NACA TN 2117, 1950.

10. McAdams, William H.: Heat Transmission. Third Ed., ch. 10, McGraw-Hill Book Co., Inc., 1954.

11. Sandborn, Virgil A., and Laurence, James C.: Heat Loss from Yawed Hot Wires at Subsonic Mach Numbers. NACA TN 3563, 1955.

12. Scadron, Marvin D., and Warshawsky, Isidore: Experimental Determination of Time Constants and Nusselt Numbers for Bare-Wire Thermocouples in High-Velocity Air Streams and Analytical Approximation of Conduction and Radiation Errors. NACA TN 2599, 1952.

13. Spangenberg, W. G.: Heat-Loss Characteristics of Hot-Wire Anemometers at Various Densities in Transonic and Supersonic Flow. NACA TN 3381, 1955.

14. Stalder, Jackson R., Goodwin, Glen, and Creager, Marcus O.: Heat Transfer to Bodies in a High-Speed Rarefied-Gas Stream. NACA Rep. 1093, 1952. (Supersedes NACA TN 2438.)

15. Winovich, Warren, and Stine, Howard A.: Measurements of the Nonlinear Variation with Temperature of Heat-Transfer Rate from Hot Wires in Transonic and Supersonic Flow. NACA TN 3965, 1957.

16. Wong, H.: Design and Development of a Free-Molecule Heat Transfer Probe. HE-150-143, Inst. Eng. Res., Univ. Calif., Oct. 15, 1956. (Contract AF-33(616)-2878.)

17. Sherman, F. S.: A Low-Density Wind-Tunnel Study of Shock-Wave Structure and Relaxation Phenomena in Gases. NACA TN 3298, 1955.

18. Hilsenrath, Joseph, et al.: Tables of Thermal Properties of Gases. Cir. 564, NBS, Nov. 1, 1955.

19. Stalder, Jackson R., Goodwin, Glen, and Creager, Marcus O.: A Comparison of Theory and Experiment for High-Speed Free-Molecule Flow. NACA Rep. 1032, 1951. (Supersedes NACA TN 2244.)

20. Kennard, Earle H.: Kinetic Theory of Gases. McGraw-Hill Book Co., Inc., 1938, pp. 312-315.

21. Corrsin, Stanley: Extended Applications of the Hot-Wire Anemometer. NACA TN 1864, 1949.

22. Leck, J. H.: Pressure Measurements in Vacuum Systems. Ch. 2 - Thermoconductivity Gages. Inst. Phys., Chapman and Hall, Ltd. (London), 1957. pp. 33-64.

23. Laurmann, J. A., and Ipsen, D. C.: Use of a Free Molecule Probe in High Speed Rarefied Gas Flow Studies. HE-150-146, Inst. Eng. Res., Univ. Calif., Apr. 30, 1957. (Contract AF-33(616)-2878.)

24. Lowell, Herman H., and Patton, Norman: Response of Homogeneous and Two-Material Laminated Cylinders to Sinusoidal Environmental Temperature Change, with Application to Hot-Wire Anemometry and Thermocouple Pyrometry. NACA TN 3514, 1955.

TABLE I. - PHYSCIAL PROPERTIES OF WIRES USED IN THIS EXPERIMENT

[Wire length = 0.50; wire diam., 2.11×10^{-4} in.; β_w, 2.67×10^{-7} $^{o}F^{-2}$.]

Probe	Ω_0, ohms	α_w, $^{o}F^{-1}$
57	42.80	1.44×10^{-3}
61	54.64	1.50×10^{-3}
63	51.40	1.53×10^{-3}
64	54.51	1.48×10^{-3}

TABLE II. - HEAT TRANSFER FROM CYLINDERS IN TRANSITION FROM SLIP FLOW TO FREE-MOLECULE FLOW

M	Kn	Re_t	T_t	T_w	Nu_t''	Nu_t	Run	M	Kn	Re_t	T_t	T_w	Nu_t''	Nu_t	Run
0.1039	0.2570	0.5899	76.0	150.0	0.3422	0.3233	29	0.2156	2.078	0.1507	78.0	150.0	0.0811	0.0715	211
				180.0	.3464	.3278	30					180.0	.0794	.0701	212
				280.0	.3491	.3315	31					280.0	.0801	.0713	213
				380.0	.3477	.3310	32					380.0	.0786	.0702	214
				480.0	.3392	.3234	33					480.0	.0705	.0686	215
				580.0	.3610	.3454	34					580.0	.0728	.0654	216
				580.0	.3403	.3246	35					180.0	.0783	.0690	217
0.1088	0.5321	0.2977	80.0	150.0	0.2233	0.2078	239	0.2172	4.022	0.0784	79.0	150.0	0.0271	0.0211	420
				180.0	.2228	.2076	240					180.0	.0223	.0168	421
				280.0	.2254	.2110	241					280.0	.0316	.0257	422
				380.0	.2280	.2143	242					380.0	.0350	.0290	423
				480.0	.2438	.2302	243					480.0	.0335	.0278	424
				580.0	.2558	.2425	244					580.0	.0414	.0355	425
				150.0	.2222	.2068	245					480.0	.0338	.0281	426
0.1094	1.045	0.1524	82.0	150.0	0.1390	0.1267	50	0.2211	4.736	0.0678	78.0	150.0	0.0430	0.0357	22
				180.0	.1355	.1236	51					180.0	.0396	.0327	23
				280.0	.1500	.1382	52					280.0	.0390	.0325	24
				380.0	.1489	.1377	53					380.0	.0338	.0279	25
				480.0	.1387	.1283	54					480.0	.0346	.0289	26
				580.0	.1576	.1471	55					580.0	.0356	.0300	27
				480.0	.1374	.1271	56					380.0	.0377	.0316	28
0.1099	2.066	0.0776	76.0	150.0	0.0980	0.0875	302	0.2225	3.508	0.0921	78.0	150.0	0.1210	0.1093	392
				180.0	.0826	.0730	303					180.0	.0830	.0734	393
				280.0	.0859	.0767	304					280.0	.0636	.0555	394
				380.0	.0862	.0774	305					380.0	.0525	.0455	395
				480.0	.0841	.0758	306					480.0	.0599	.0527	396
				580.0	.0830	.0751	307					580.0	.0566	.0499	397
				480.0	.0867	.0783	308					480.0	.0600	.0528	398
0.1101	0.1074	1.491	83.0	150.0	0.3002	0.2823	176	0.3015	1.00[illegible]	0.4343	80.0	150.0	0.1513	0.1443	358
				180.0	.3063	.2887	177					180.0	.1548	.1421	359
				280.0	.3330	.3156	178					280.0	.1589	.1467	360
				380.0	.4081	.3899	179					380.0	.1552	.1438	361
				480.0	.4550	.4367	180					480.0	.1504	.1396	362
				580.0	.5205	.5018	181					580.0	.1611	.1504	363
				580.0	.3275	.3125	182					180.0	.1523	.1337	364
0.1233	3.474	0.0517	77.0	150.0	0.1200	0.1084	113	0.3111	0.2606	1.717	87.0	150.0	0.4113	0.3907	463
				180.0	.0826	.0730	114					180.0	.4162	.3959	464
				280.0	.0604	.0525	115					280.0	.4163	.3978	465
				380.0	.0500	.0431	116					380.0	.4360	.4174	466
				480.0	.0580	.0509	117					480.0	.4400	.4222	467
				580.0	.0562	.0495	118					580.0	.4436	.4264	468
				180.0	.0854	.0757	119					180.0	.4347	.4140	469
0.2119	0.1049	2.927	84.0	150.0	0.6593	0.6332	281	0.3139	0.10[illegible]6	4.281	84.0	150.0	0.7191	0.6920	99
				180.0	.6731	.6473	282					180.0	.7387	.7118	100
				280.0	.6962	.6716	283					280.0	.7553	.7296	101
				380.0	.6992	.6758	284					380.0	.7457	.7216	102
				480.0	.6820	.6600	285					480.0	.7363	.7135	103
				580.0	.6850	.6642	286					580.0	.7347	.7129	104
				580.0	.6807	.6597	287					480.0	.7382	.7153	105
0.2121	0.1076	2.853	85.0	150.0	0.6592	0.6340	78	0.3141	0.10[illegible]7	4.160	86.5	147.0	0.7171	0.6909	162
				179.5	.6727	.6478	79					179.45	.7288	.7030	163
				283.8	.6889	.6654	80					283.95	.7485	.7240	164
				385.0	.6954	.6730	81					383.95	.7469	.7237	165
				486.5	.6920	.6708	82					486.45	.7426	.7206	166
				584.5	.6920	.6718	83					584.45	.7407	.7198	167
				385.0	.6911	.6688	84					486.45	.7408	.7189	168
	0.2609	1.177	85.0	154.9	0.3917	0.3714	323	0.3144	1.05[illegible]	0.4318	82.0	150.0	0.1574	0.1444	470
				187.9	.3851	.3654	324					180.0	.1547	.1420	471
				286.9	.3855	.3698	325					280.0	.1586	.1464	472
				385.9	.4077	.3895	326					380.0	.1549	.1435	473
				483.9	.4271	.4093	327					480.0	.1500	.1392	474
				581.9	.4315	.4144	328					580.0	.1607	.1500	475
				286.9	.3997	.3807	329					180.0	.1522	.1396	476
0.2151	1.049	0.2971	82.0	150.0	0.1514	0.1386	141	0.3157	2.07[illegible]	0.2199	76.0	180.0	0.0794	0.0701	225
				180.0	.1465	.1341	142					280.0	.0836	.0746	226
				280.0	.1588	.1467	143					380.0	.0858	.0771	227
				380.0	.1535	.1421	144					480.0	.0919	.0833	228
				480.0	.1448	.1342	145					580.0	.0940	.0857	229
				580.0	.1593	.1486	146					380.0	.0915	.0825	230
				580.0	.1604	.1498	147								

TABLE II. - Continued. HEAT TRANSFER FROM CYLINDERS IN TRANSITION FROM SLIP FLOW TO FREE-MOLECULE FLOW

M	Kn	Re_t	T_t	T_w	Nu_t''	Nu_t	Run	M	Kn	Re_t	T_t	T_w	Nu_t''	Nu_t	Run
0.3165	0.5267	0.8655	84.0	150.0	0.2897	0.2720	441	0.4246	2.110	0.2880	81.0	150.0	0.1016	0.0910	253
				180.0	.2836	.2665	442					180.0	.0955	.0854	254
				280.0	.2789	.2629	443					280.0	.0933	.0838	255
				380.0	.2755	.2604	444					380.0	.0900	.0812	256
				480.0	.2765	.2621	445					480.0	.0921	.0836	257
				580.0	.2762	.2644	446					580.0	.0871	.0791	258
				380.0	.2253	.2153	447					380.0	.0923	.0833	259
0.3278	3.517	0.1346	77.5	150.0	0.1204	0.1088	477	0.4283	3.495	0.1756	78.0	150.0	0.1241	0.1123	120
				180.0	.0841	.0745	478					180.0	.0852	.0755	121
				280.0	.0596	.0518	479					280.0	.0636	.0555	122
				380.0	.0525	.0454	480					380.0	.0561	.0488	123
				480.0	.0605	.0533	481					480.0	.0623	.0550	124
				580.0	.0576	.0508	482					580.0	.0581	.0515	125
				280.0	.0582	.0512	483					280.0	.0636	.0554	126
0.3281	4.720	0.1004	77.0	150.0	0.0328	0.0263	267	0.5085	1.053	0.6855	82.0	150.0	0.2136	0.1984	246
				180.0	.0349	.0284	268					180.0	.2015	.1871	247
				280.0	.0373	.0308	269					280.0	.1892	.1759	248
				380.0	.0373	.0311	270					380.0	.1733	.1612	249
				480.0	.0372	.0313	271					480.0	.1696	.1582	250
				580.0	.0368	.0311	272					580.0	.1813	.1700	251
				380.0	.0373	.0311	273					580.0	.1816	.1703	252
0.3287	4.033	0.1175	80.0	150.0	0.0252	0.0194	456		1.045	0.6920	78.0	150.0	0.1739	0.1603	85
				180.0	.0320	.0256	457					180.0	.1738	.1604	86
				280.0	.0376	.0311	458					280.0	.1755	.1628	87
				380.0	.0398	.0335	459					380.0	.1651	.1534	88
				480.0	.0408	.0347	460					480.0	.1637	.1526	89
				580.0	.0425	.0365	461					580.0	.1765	.1654	90
				480.0	.0406	.0345	462					580.0	.1768	.1657	91
0.4051	0.2575	2.249	86.0	155.0	0.5098	0.4869	1	0.5114	0.1078	6.7323	83.0	385.0	0.8519	0.8272	235
				188.0	.4923	.4703	2					486.5	.8447	.8213	236
				287.0	.4655	.4452	3					584.5	.8541	.8316	237
				386.0	.4709	.4516	4								
				484.0	.4630	.4447	5								
				582.0	.4597	.4422	6								
				582.0	.4621	.4446	7								
0.4125	1.040	0.5696	75.0	150.0	0.1579	0.1448	183	0.5151	0.2780	2.6929	86.0	147.0	0.4625	0.4413	330
				180.0	.1658	.1526	184					179.5	.4693	.4485	331
				280.0	.1600	.1478	185					284.0	.4832	.4634	332
				380.0	.1580	.1464	186					385.0	.4768	.4582	333
				480.0	.1555	.1445	187					486.5	.4668	.4492	334
				580.0	.1677	.1568	188					584.5	.4655	.4464	335
				380.0	.1568	.1453	189					284.0	.4796	.4599	336
0.4146	0.1074	5.524	82.0	147.0	0.7358	0.7093	344	0.5165	0.2643	2.7663	86.0	155.0	0.4896	0.4672	36
				179.4	.7627	.7362	345					188.0	.4818	.4601	37
				283.9	.8072	.7817	346					287.0	.4656	.4454	38
				384.9	.8009	.7769	347					386.0	.4730	.4538	39
				486.4	.8063	.7834	348					484.0	.4670	.4487	40
				584.4	.8149	.7929	349					581.0	.4622	.4448	41
				584.4	.8068	.7849	350					484.0	.4641	.4459	42
0.4147	0.5273	1.125	83.0	150.0	0.2974	0.2794	57	0.5231	2.095	0.3548	77.0	150.0	0.0855	0.0756	148
				180.0	.2956	.2781	58					180.0	.0860	.0768	149
				280.0	.2955	.2790	59					280.0	.1012	.0912	150
				380.0	.2879	.2724	60					380.0	.1003	.0909	151
				480.0	.2886	.2738	61					480.0	.0955	.0867	152
				580.0	.2869	.2728	62					580.0	.0956	.0871	153
				380.0	.2886	.2731	63					380.0	.1446	.1335	154
0.4165	0.2714	2.190	87.5	147.0	0.4373	0.4168	372	0.5248	4.699	0.1588	75.5	150.0	0.0460	0.0384	427
				179.4	.4454	.4251	373					180.0	.0455	.0381	428
				283.9	.4534	.4343	374					280.0	.0458	.0388	429
				384.9	.4484	.4304	375					380.0	.0458	.0390	430
				486.4	.4410	.4240	376					480.0	.0451	.0386	431
				584.4	.4388	.4226	377					580.0	.0442	.0381	432
												380.0	.0456	.0388	433
0.4186	4.706	0.1276	77.0	150.0	0.0314	0.0249	406	0.5250	0.5268	1.4112	84.0	150.0	0.3090	0.2909	309
				180.0	.0360	.0293	407					180.0	.3168	.2989	310
				280.0	.0428	.0353	408					280.0	.3066	.2899	311
				380.0	.0423	.0358	409					380.0	.3063	.2905	312
				480.0	.0422	.0359	410					480.0	.3138	.2986	313
				580.0	.0417	.0357	411					580.0	.3146	.2900	314
				380.0	.0445	.0378	412					380.0	.3007	.2850	315

TABLE II. - Continued. HEAT TRANSFER FROM CYLINDERS IN TRANSITION FROM SLIP FLOW TO FREE-MOLECULE FLOW

M	Kn	Re_t	T_t	T_w	Nu_t''	Nu_t	Run
0.5279	3.484	0.2151	78.0	150.0	0.1235	0.1117	399
				180.0	.0900	.0800	400
				280.0	.0660	.0578	401
				380.0	.0591	.0516	402
				480.0	.0633	.0559	403
				580.0	.0593	.0524	404
				380.0	.0591	.0517	405
0.6036	2.062	0.4125	77.5	150.0	0.0912	0.0811	365
				180.0	.0965	.0863	366
				280.0	.0941	.0845	367
				380.0	.0958	.0866	368
				480.0	.0943	.0855	369
				580.0	.0927	.0844	370
				480.0	.0958	.0870	371
0.6079	0.1086	7.854	85.5	150.0	0.8520	0.8235	106
				180.0	.8720	.8438	107
				280.0	.8727	.8463	108
				380.0	.8379	.8136	109
				480.0	.8434	.8202	110
				580.0	.8300	.8080	111
				480.0	.8240	.8011	112
0.6146	1.054	0.8187	82.0	150.0	0.1607	0.1475	295
				180.0	.1667	.1534	296
				280.0	.1687	.1561	297
				380.0	.1666	.1547	298
				480.0	.1650	.1537	299
				580.0	.1827	.1713	300
				380.0	.1666	.1547	301
0.6163	4.052	0.2135	82.0	150.0	0.0417	0.0344	169
				180.0	.0465	.0390	170
				280.0	.0522	.0447	171
				380.0	.0528	.0456	172
				480.0	.0519	.0451	173
				580.0	.0519	.0453	174
				180.0	.0489	.0412	175
0.6222	4.722	0.1852	78.0	150.0	0.0504	0.0425	204
				180.0	.0506	.0428	205
				280.0	.0503	.0430	206
				380.0	.0501	.0430	207
				480.0	.0490	.0423	208
				580.0	.0484	.0420	209
				480.0	.0516	.0448	210
0.6240	3.465	0.2522	76.0	150.0	0.1230	0.1113	15
				180.0	.0882	.0783	16
				280.0	.0694	.0610	17
				380.0	.0679	.0599	18
				480.0	.0654	.0579	19
				580.0	.0643	.0571	20
				380.0	.0670	.0591	21
0.6851	0.1095	8.684	88.0	147.0	0.8845	0.8555	274
				179.5	.9093	.8806	275
				284.0	.9295	.9093	276
				385.0	.9122	.8868	277
				486.5	.9138	.8896	278
				584.5	.8898	.8670	279
				584.5	.8898	.8670	280
0.6871	0.2663	3.583	86.0	155.0	0.5287	0.5055	127
				188.0	.5209	.4984	128
				287.0	.5036	.4827	129
				386.0	.5066	.4867	130
				484.0	.4979	.4791	131
				582.0	.4910	.4731	132
				386.0	.5015	.4817	133
0.7042	0.5416	1.802	86.0	147.0	0.3034	0.2861	351
				189.5	.3080	.2910	352
				284.0	.3173	.3011	353
				385.0	.3102	.2951	354
				486.5	.3030	.2887	355
				584.5	.3131	.2993	356
				486.5	.3041	.2898	357

M	Kn	Re_t	T_t	T_w	Nu_t''	Nu_t	Run
0.7063	2.091	0.4700	78.0	150.0	0.1023	0.0916	413
				180.0	.1058	.0951	414
				280.0	.1064	.0963	415
				380.0	.1020	.0925	416
				480.0	.0999	.0909	417
				580.0	.0977	.0892	418
				280.0	.1028	.0928	419
	2.102	0.4667	81.0	150.0	0.1171	0.1056	190
				180.0	.1162	.1050	191
				280.0	.1113	.1009	192
				380.0	.1050	.0953	193
				480.0	.1019	.0928	194
				580.0	.1002	.0892	195
				180.0	.1162	.1048	196
0.7096	3.476	0.2839	78.0	150.0	0.1290	0.1170	434
				180.0	.0911	.0811	435
				280.0	.0729	.0643	436
				380.0	.0727	.0645	437
				480.0	.0747	.0668	438
				580.0	.0689	.0616	439
				380.0	.0721	.0640	440
	4.722	0.2089	78.0	150.0	0.0459	0.0383	64
				180.0	.0490	.0413	65
				280.0	.0525	.0449	66
				380.0	.0527	.0455	67
				480.0	.0513	.0445	68
				580.0	.0514	.0449	69
				280.0	.0524	.0449	70
0.7131	4.000	0.2478	78.0	150.0	0.0469	0.0392	449
				180.0	.0521	.0442	450
				280.0	.0566	.0489	451
				380.0	.0564	.0491	452
				480.0	.0557	.0487	453
				580.0	.0559	.0491	454
				280.0	.0563	.0489	455
0.7177	1.053	0.9453	82.0	150.0	0.1699	0.1563	378
				180.0	.1665	.1534	379
				280.0	.1732	.1604	380
				380.0	.1717	.1597	381
				480.0	.1689	.1574	382
				580.0	.1871	.1756	383
				480.0	.1688	.1573	384
0.7722	1.061	1.002	81.0	150.0	0.1793	0.1653	218
				180.0	.1766	.1630	219
				280.0	.1802	.1672	220
				380.0	.1785	.1662	221
				480.0	.1751	.1635	222
				580.0	.1910	.1794	223
				380.0	.1790	.1667	224
0.7882	0.[illegible]085	9.965	84.0	147.0	0.8773	0.8483	155
				179.5	.9702	.9405	156
				284.0	.9780	.9500	157
				375.0	.9567	.9306	158
				486.5	.9511	.9263	159
				584.5	.9631	.9393	160
				284.0	.9934	.9652	161
0.7938	2.[illegible]11	0.5171	77.5	150.0	0.0977	0.0872	92
				180.0	.1013	.0908	93
				280.0	.1044	.0944	94
				380.0	.1027	.0932	95
				480.0	.1008	.0918	96
				580.0	.0995	.0909	97
				280.0	.1040	.0940	98
0.7975	4.[illegible]05	0.2330	77.0	150.0	0.0567	0.0482	337
				180.0	.0564	.0482	338
				280.0	.0565	.0488	339
				380.0	.0556	.0483	340
				480.0	.0568	.0497	341
				580.0	.0536	.0469	342
				280.0	.0560	.0483	343

TABLE II. - Concluded. HEAT TRANSFER FROM CYLINDERS IN TRANSITION FROM SLIP FLOW TO FREE-MOLECULE FLOW

M	Kn	Re_t	T_t	T_w	Nu_t''	Nu_t	Run	M	Kn	Re_t	T_t	T_w	Nu_t''	Nu_t	Run
0.7979	3.506	0.3127	78.0	150.0	0.1389	0.1264	288	0.8674	0.2641	4.446	87.0	155.0	0.5705	0.5465	71
				180.0	.0975	.0871	289					188.0	.5579	.5347	72
				280.0	.0784	.0695	290					287.0	.5294	.5080	73
				380.0	.0757	.0674	291					386.0	.5260	.5057	74
				480.0	.0749	.0669	292					484.0	.5171	.4980	75
				580.0	.0741	.0665	293					582.0	.5463	.5275	76
				280.0	.0782	.0693	294					582.0	.5437	.5249	77
0.8104	0.2765	4.008	84.5	147.0	0.5353	0.5127	8	0.8733	0.1096	10.781	87.0	147.0	0.9865	0.9559	197
				179.5	.5386	.5163	9					179.5	.9928	.9628	198
				184.0	.5315	.5179	10					284.0	1.0074	.9792	199
				385.0	.5201	.5120	11					385.0	1.0002	.9735	200
				486.5	.5409	.5018	12					486.5	.9882	.9631	201
				584.5	.5201	.5231	13					584.5	1.0307	1.0061	202
				486.5	.5201	.5018	14					284.0	1.0047	.9764	203
0.8268	4.006	0.2823	79.0	150.0	0.0410	0.0337	385	0.8863	3.502	0.3432	78.0	150.0	0.1499	0.1369	260
				180.0	.0648	.0561	386					180.0	.1046	.0938	261
				280.0	.0652	.0561	387					280.0	.0818	.0726	262
				380.0	.0643	.0569	388					380.0	.0801	.0715	263
				480.0	.0628	.0565	389					480.0	.0794	.0712	264
				580.0	.0623	.0554	390					580.0	.0781	.0703	265
				380.0	.0639	.0561	391					380.0	.0782	.0697	266
0.8363	2.027	0.5639	78.0	150.0	0.1110	0.0998	316	0.8871	4.028	0.2991	75.0	150.0	0.0459	0.0382	134
				180.0	.1175	.1062	317					180.0	.0678	.0588	135
				280.0	.1123	.1020	318					280.0	.0702	.0616	136
				380.0	.1108	.1010	319					380.0	.0690	.0609	137
				480.0	.1079	.0987	320					480.0	.0667	.0590	138
				580.0	.1062	.0974	321					580.0	.0660	.0587	139
				280.0	.1115	.1012	322					280.0	.0686	.0601	140
0.8668	0.5417	2.166	87.5	147.0	0.3323	0.3143	43								
				179.5	.3371	.3194	44								
				284.0	.3418	.3250	45								
				385.0	.3380	.3223	46								
				486.5	.3339	.3190	47								
				484.5	.3323	.3181	48								
				385.0	.3385	.3227	49								

TABLE III. - DIMENSIONLESS FUNCTIONS

Mach number, M	s	g(s)	f(s)	$\frac{T_{e,\infty}}{T_t}$
0.05	0.042	9.43323	9.44172	1.0004
.10	.084	9.45858	9.49210	1.0015
.15	.126	9.49908	9.57430	1.0034
.20	.167	9.55632	9.68872	1.0058
.25	.209	9.63015	9.83834	1.0091
.30	.251	9.71958	10.02114	1.0128
.35	.293	9.82485	10.23799	1.0171
.40	.335	9.94602	10.48942	1.0219
.45	.377	10.08321	10.77637	1.0272
.50	.418	10.22958	11.08815	1.0323
.55	.460	10.39665	11.44568	1.0381
.57	.477	10.46736	11.59930	1.0405
.59	.494	10.54086	11.75943	1.0430
.61	.511	10.61694	11.92605	1.0455
.63	.527	10.69080	12.08838	1.0476
.65	.544	10.76952	12.26456	1.0501
.67	.561	10.85100	12.44746	1.0526
.69	.578	10.93728	12.63973	1.0552
.71	.594	11.01711	12.82192	1.0572
.73	.611	11.10813	13.02687	1.0598
.75	.628	11.19696	13.23293	1.0623
.77	.644	11.28270	13.43252	1.0643
.79	.661	11.37807	13.65378	1.0668
.80	.670	11.42904	13.77319	1.0683
.85	.711	11.66832	14.33964	1.0737
.90	.753	11.92563	14.96017	1.0796
.95	.795	12.19029	15.61611	1.0852
1.00	.837	12.46626	16.31451	1.0905

TABLE IV. - MEASURED RECOVERY TEMPERATURES

T_e/T_t	$T_e/T_{e,\infty}$	M	Kn
0.9839	0.9615	0.4138	1.052
.9826	.9511	.5080	1.051
1.000	0.9982	0.1097	2.078
.9982	.9916	.2162	2.082
.9938	.9800	.3160	2.088
.9894	.9660	.4231	2.102
.9850	.9520	.5219	2.103
.9850	.9421	.6131	2.092
.9901	.9367	.7041	2.096
.9863	.9235	.7935	2.117
.9750	.9058	.8682	2.113
0.9938	0.9915	0.1214	3.487
.9976	.9906	.2221	3.514
.9964	.9817	.3258	3.527
.9989	.9746	.4299	3.507
.9995	.9654	.5269	3.492
.9989	.9542	.6231	3.501
1.007	.9526	.7059	3.486
1.011	.9461	.7979	3.519
1.019	.9453	.8846	3.511
0.9912	0.9845	0.2170	4.007
.9969	.9820	.3291	4.010
.9944	.9707	.4154	4.013
1.010	.9754	.5306	3.999
1.019	.9738	.6157	4.015
1.029	.9727	.7134	4.000
1.042	.9723	.8261	3.992
1.054	.9775	.8887	4.041
0.9949	0.9881	0.2207	4.710
1.009	.9939	.3274	4.703
1.017	.9931	.4170	4.689
1.029	.9937	.5260	4.694
1.040	.9933	.6210	4.697
1.049	.9921	.7083	4.698
1.056	.9889	.7953	4.682
1.067	.9901	.8836	4.774

TABLE V. - ACCOMMODATION COEFFICIENT CALCULATED USING MEASURED NUSSELT NUMBERS AND FREE-MOLECULE-FLOW PREDICTION (EQ. (13))

M	$Nu_{t,meas}$	Kn	α_{calc}
0.5248	0.03808	4.6994	0.545
.7975	.04694	4.7051	.655
.3281	.03110	4.7199	.482
.8901	.05322	4.8001	.776
.2211	.03001	4.7359	.472
.7095	.04486	4.7225	.638
.4186	.03565	4.7058	.545
.6222	.04196	4.7218	.616
.5311	.04203	4.0135	.532
.8268	.05514	4.0064	.654
.2172	.03550	4.0223	.496
.8871	.05866	4.0283	.706
.4270	.03800	4.0050	.488
.7131	.04900	4.0001	.597
.3287	.03650	4.0330	.482
.6163	.04530	4.0520	.572
			$\alpha_{av} = 0.57$

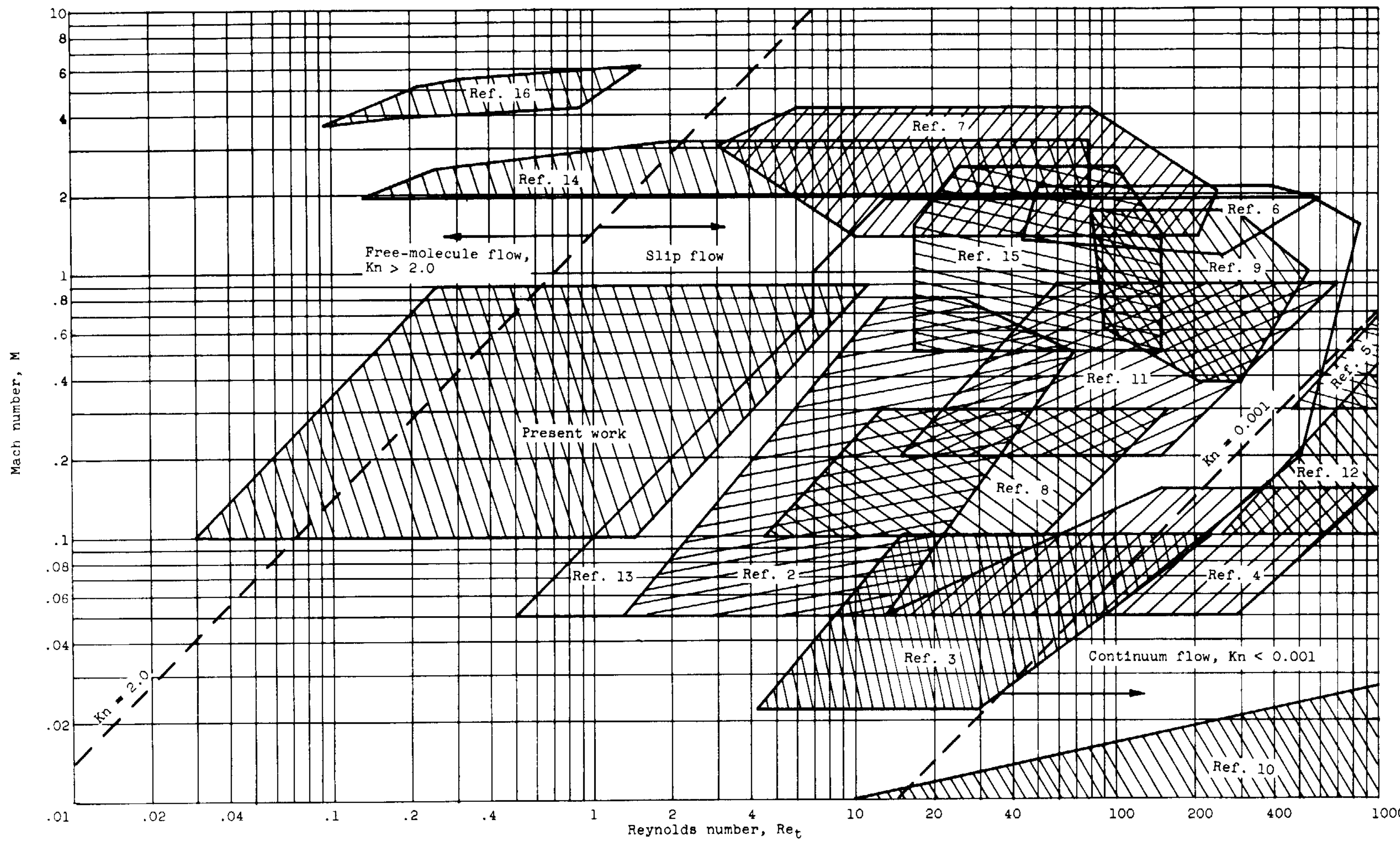

Figure 1. - Comparison of Mach and Reynolds number ranges of heat-transfer experiments for previous and present work.

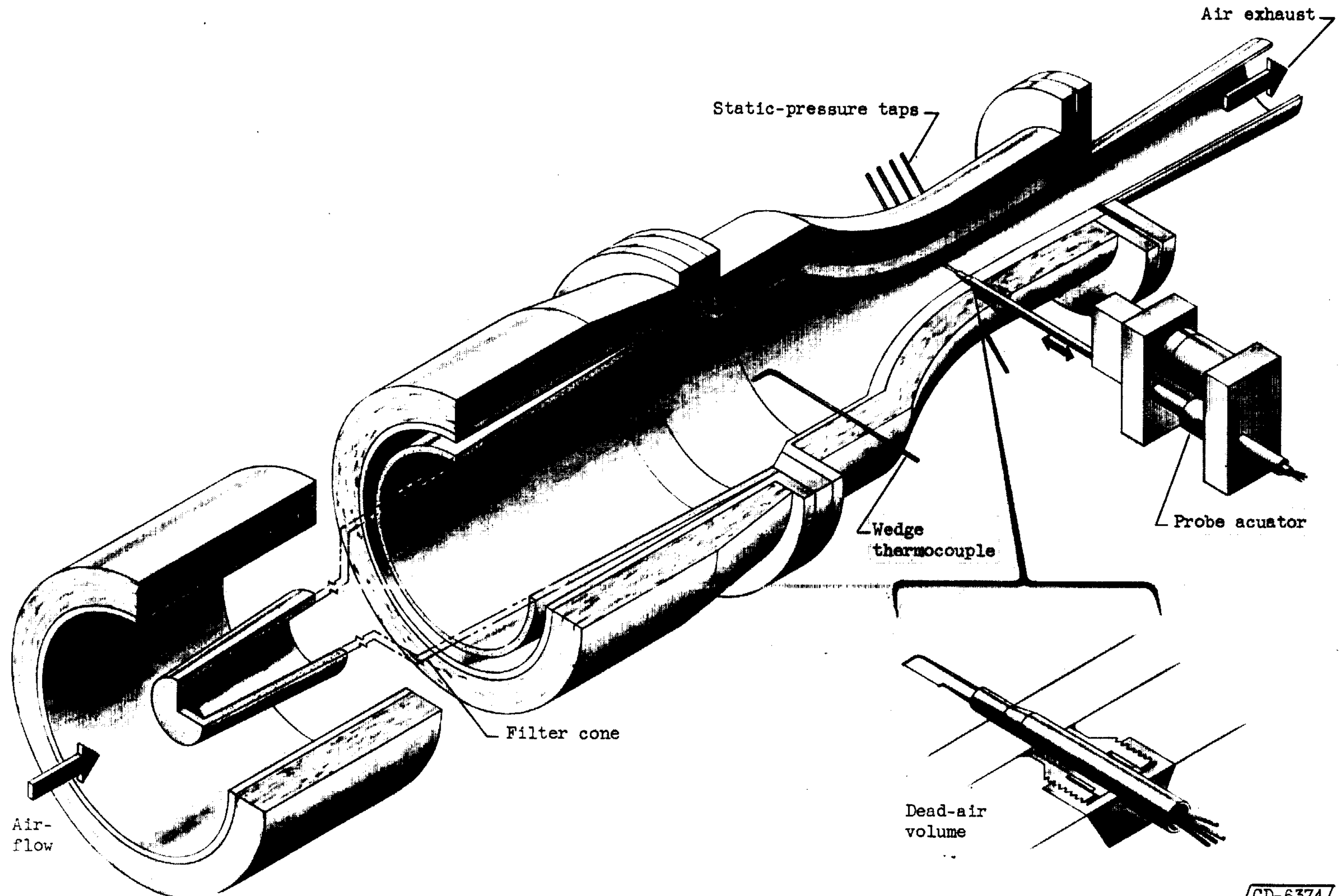

Figure 2. - Variable-density subsonic tunnel.

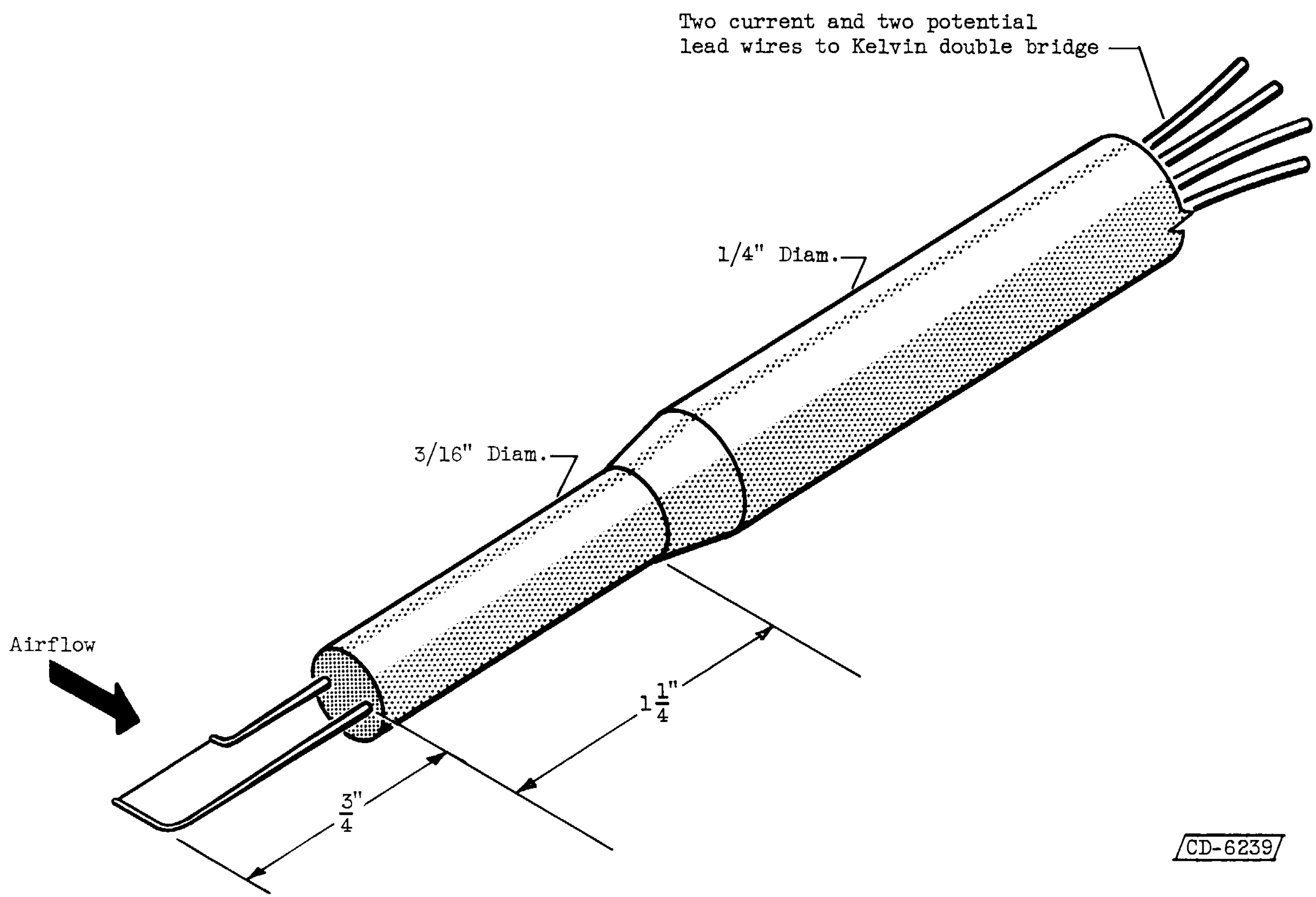

Figure 3. - Tungsten-wire supporting probe.

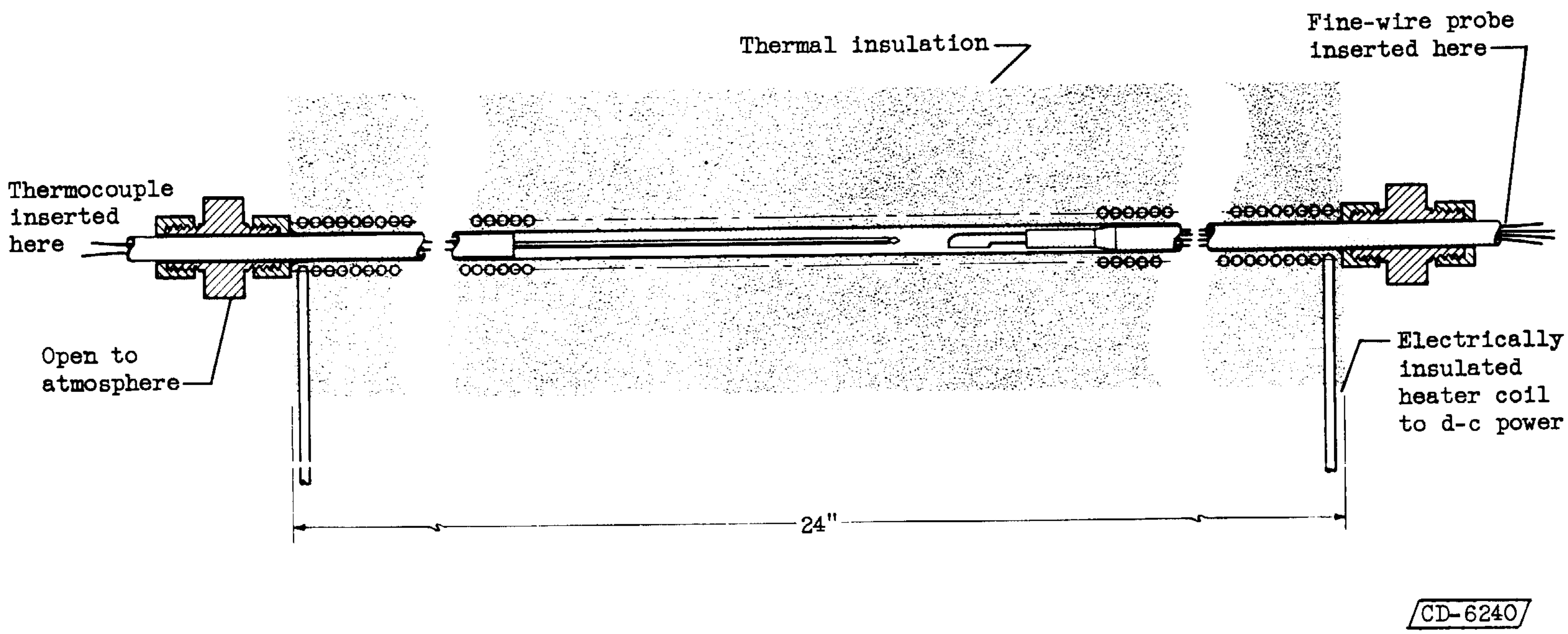

Figure 4. - Resistance-temperature calibration tank.

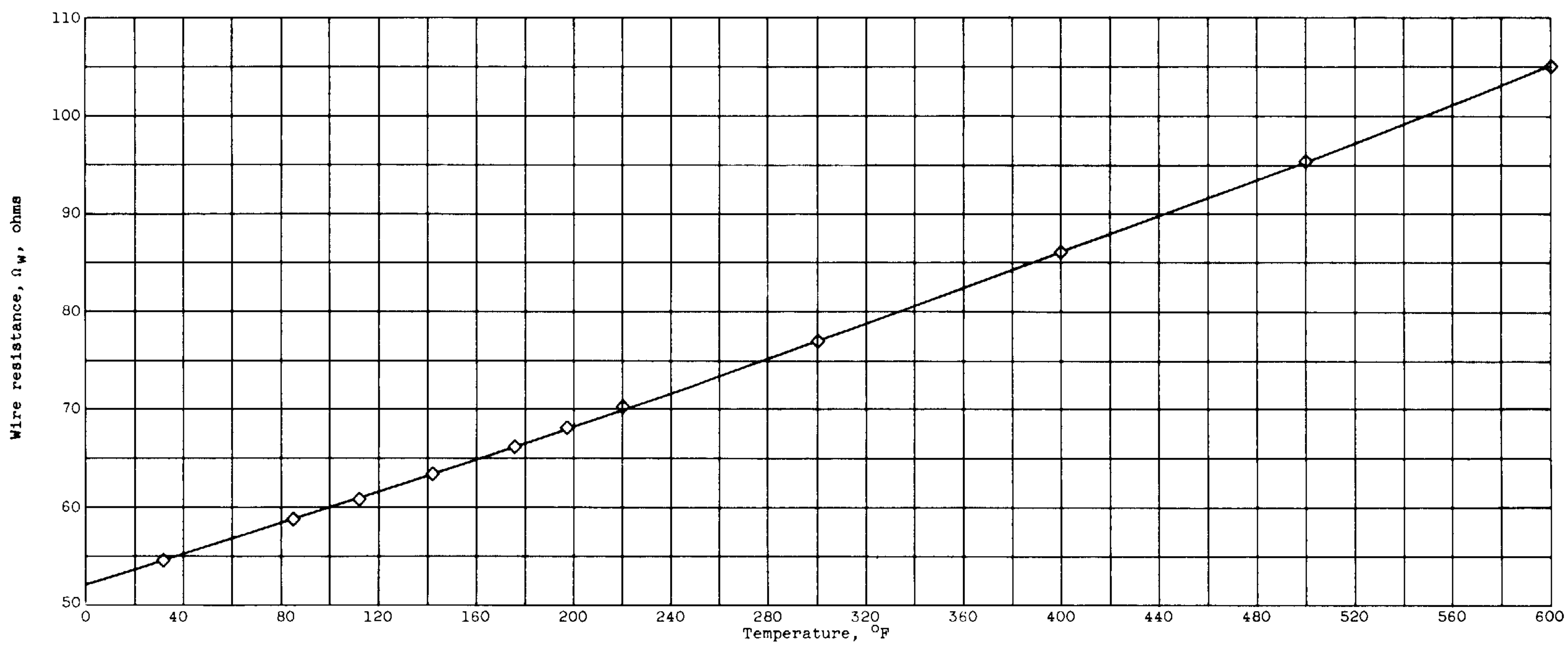

Figure 5. - Calibration of wire electrical resistance and temperature of probe 64; Ω_0 = 54.5 ohms; $\alpha_w = 1.48\times10^{-3}$ °F^{-1}; $\beta_w = 2.67\times10^{-7}$ °F^{-2}.

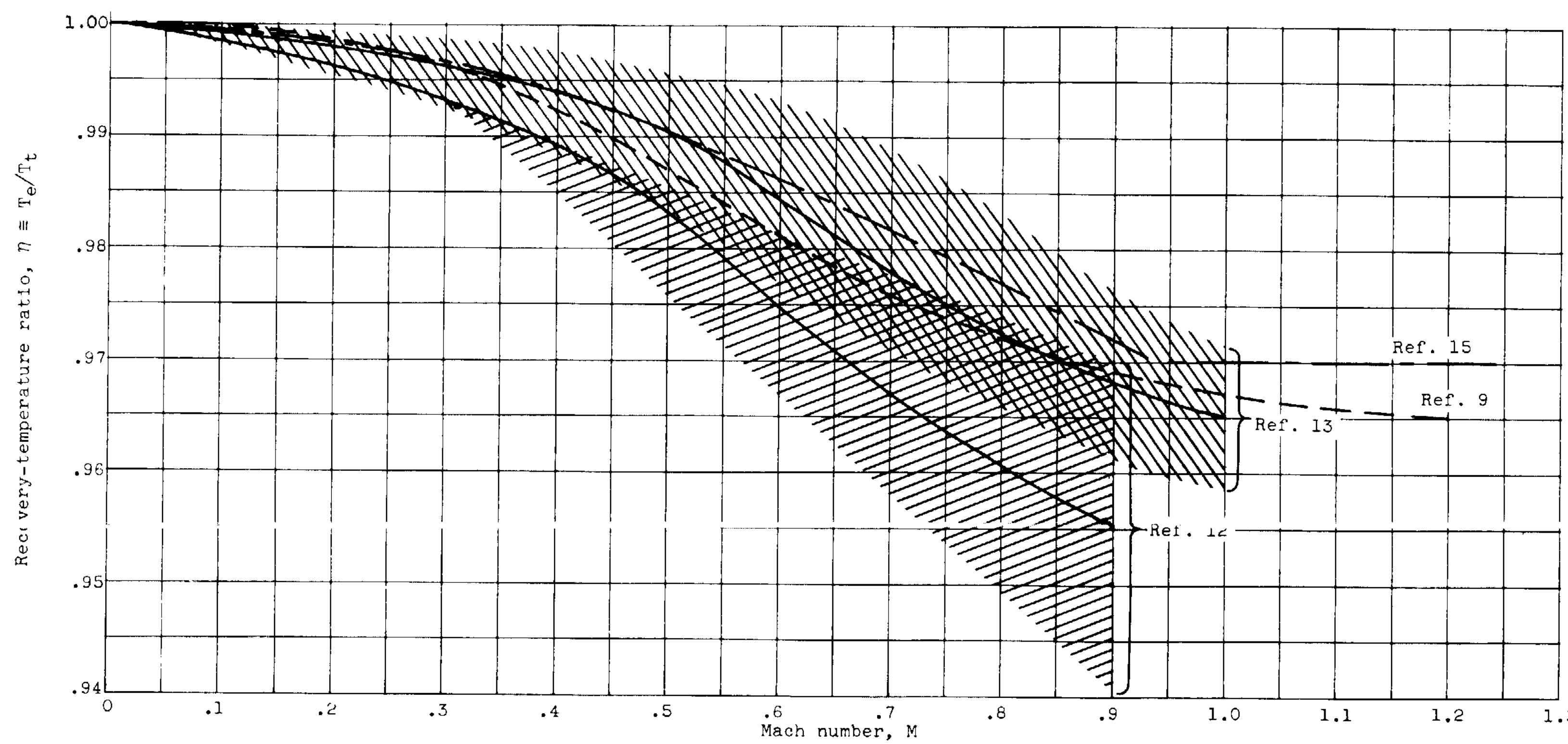

Figure 6. - Previous subsonic data on recovery temperature for Knudsen number less than 0.1.

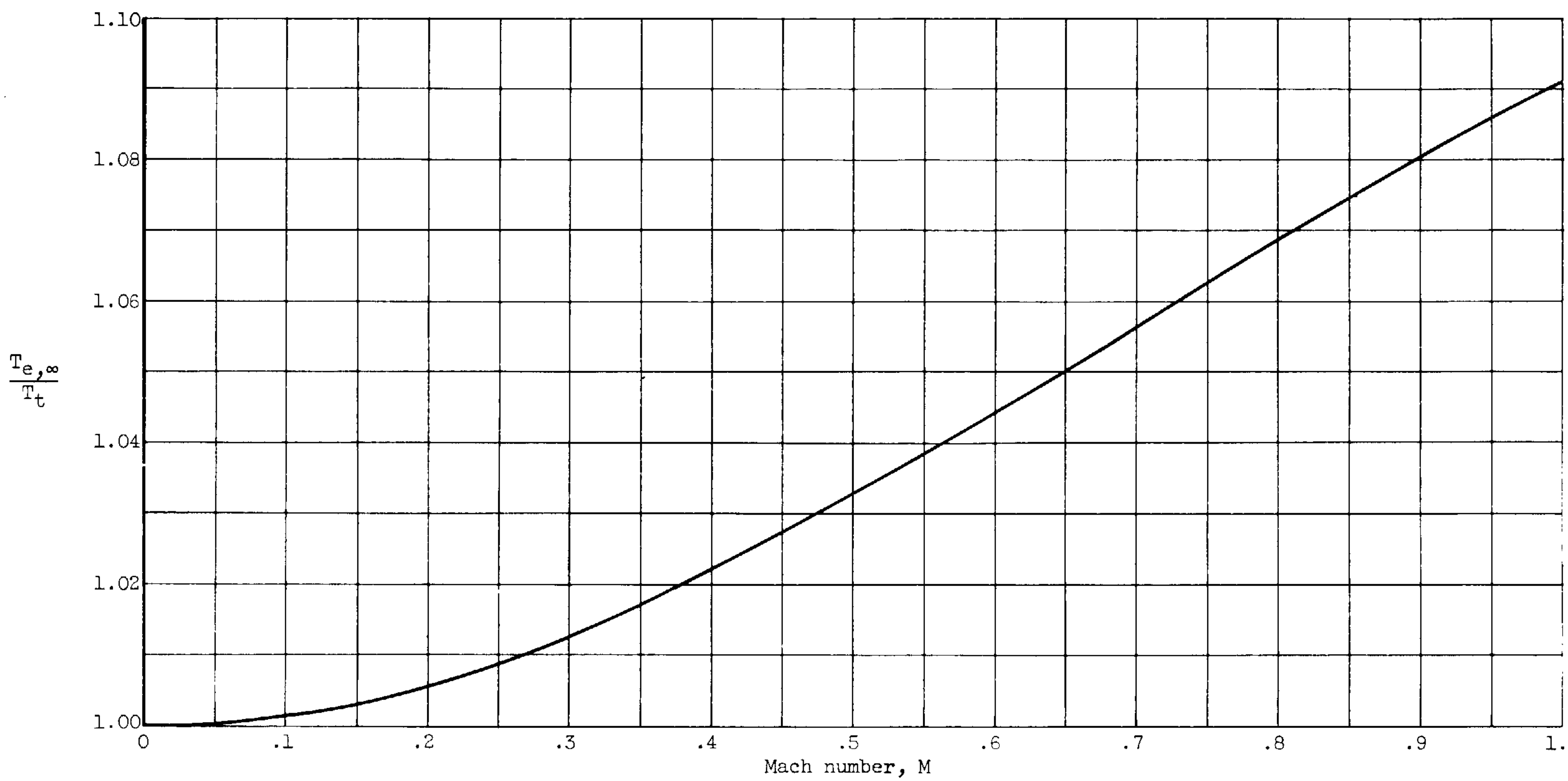

Figure 7. - Predicted curve from free-molecule-flow theory (eq. (8)).

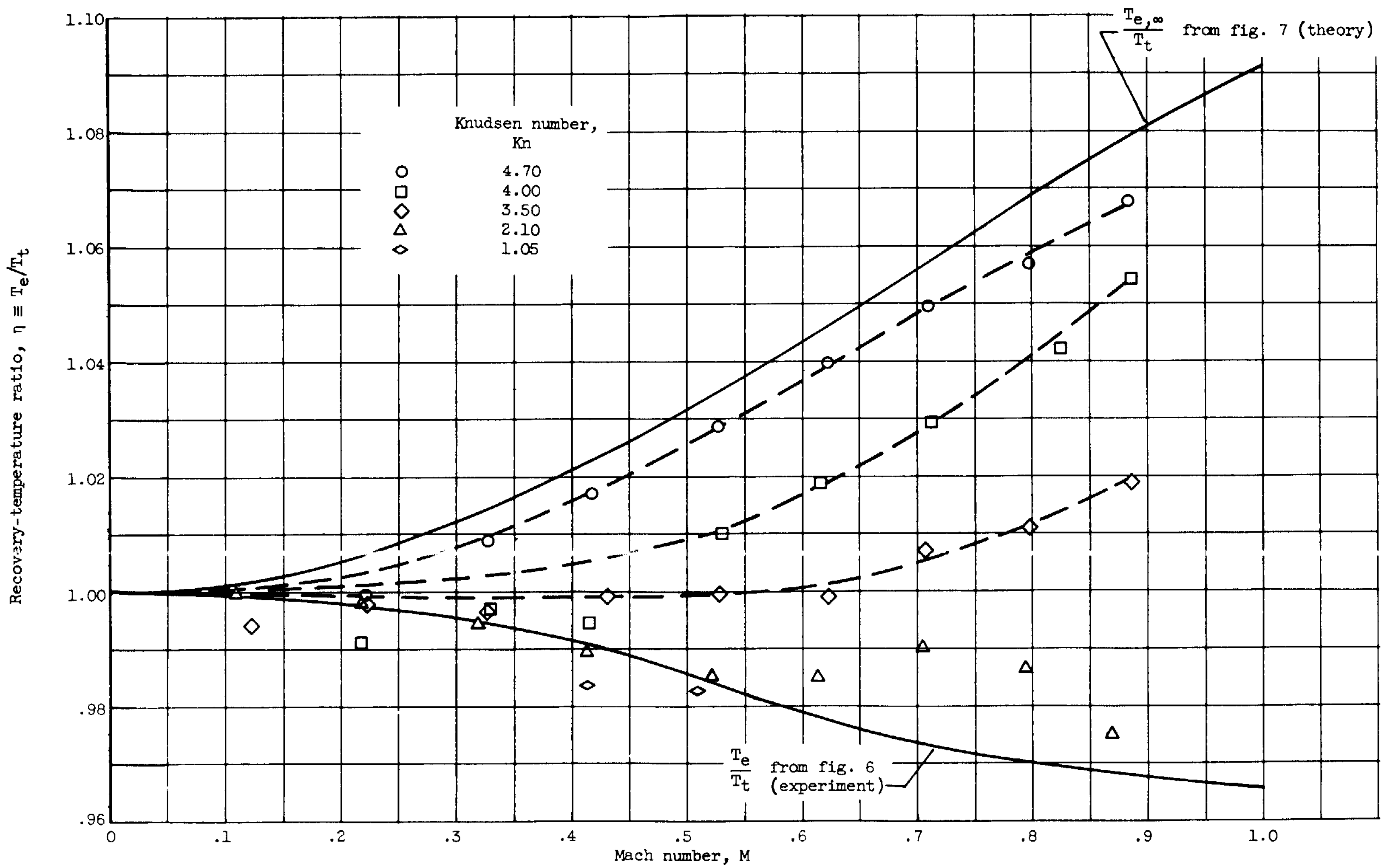

Figure 8. - Data of this research compared with previous data and theory.

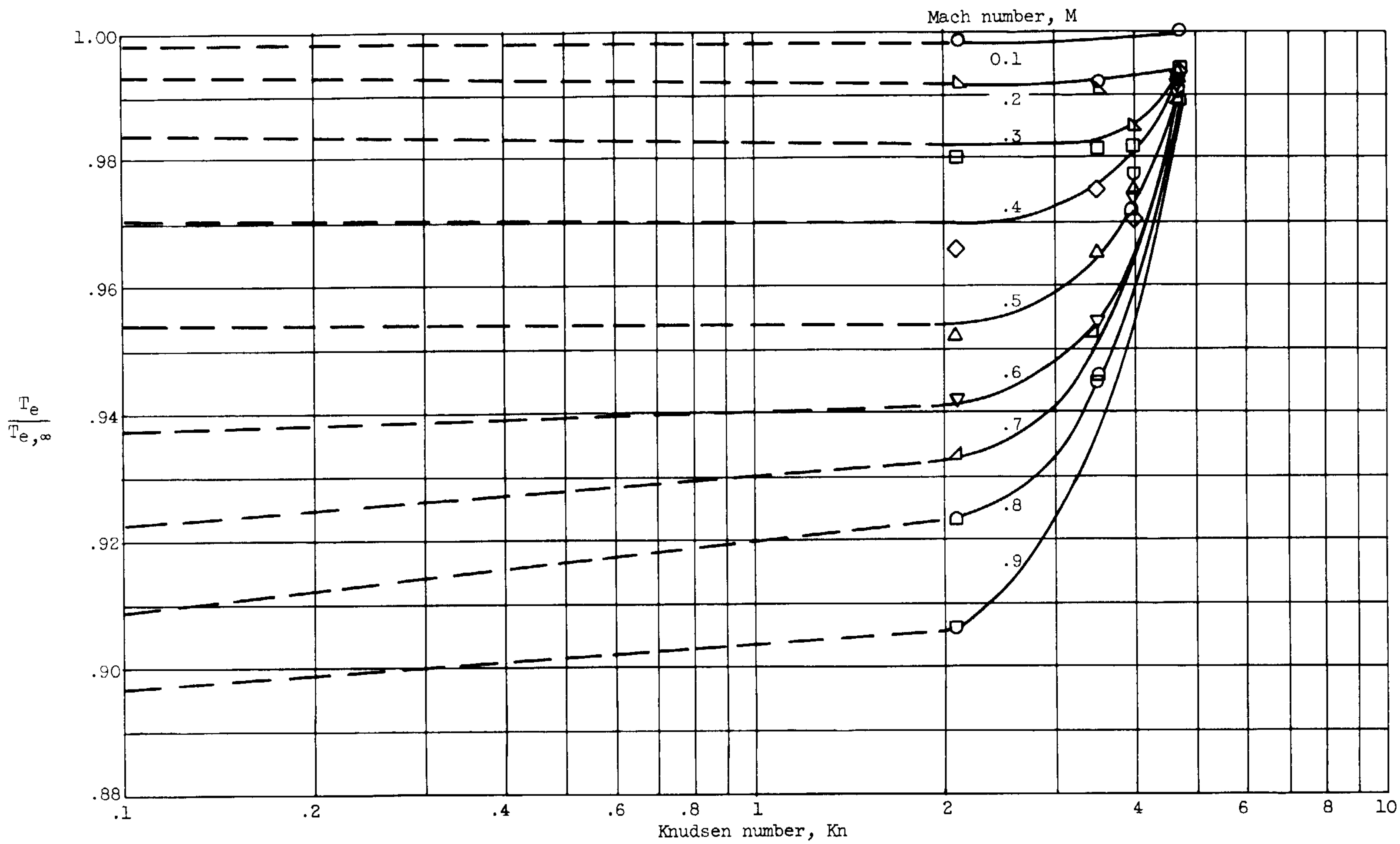

Figure 9. - Variation of ratio of measured to theoretical equilibrium temperature with free-stream Knudsen number for transverse cylinders. (Values of $T_e/T_{e,\infty}$ at Kn = 0.1 are from fig. 6 (ref. 9).)

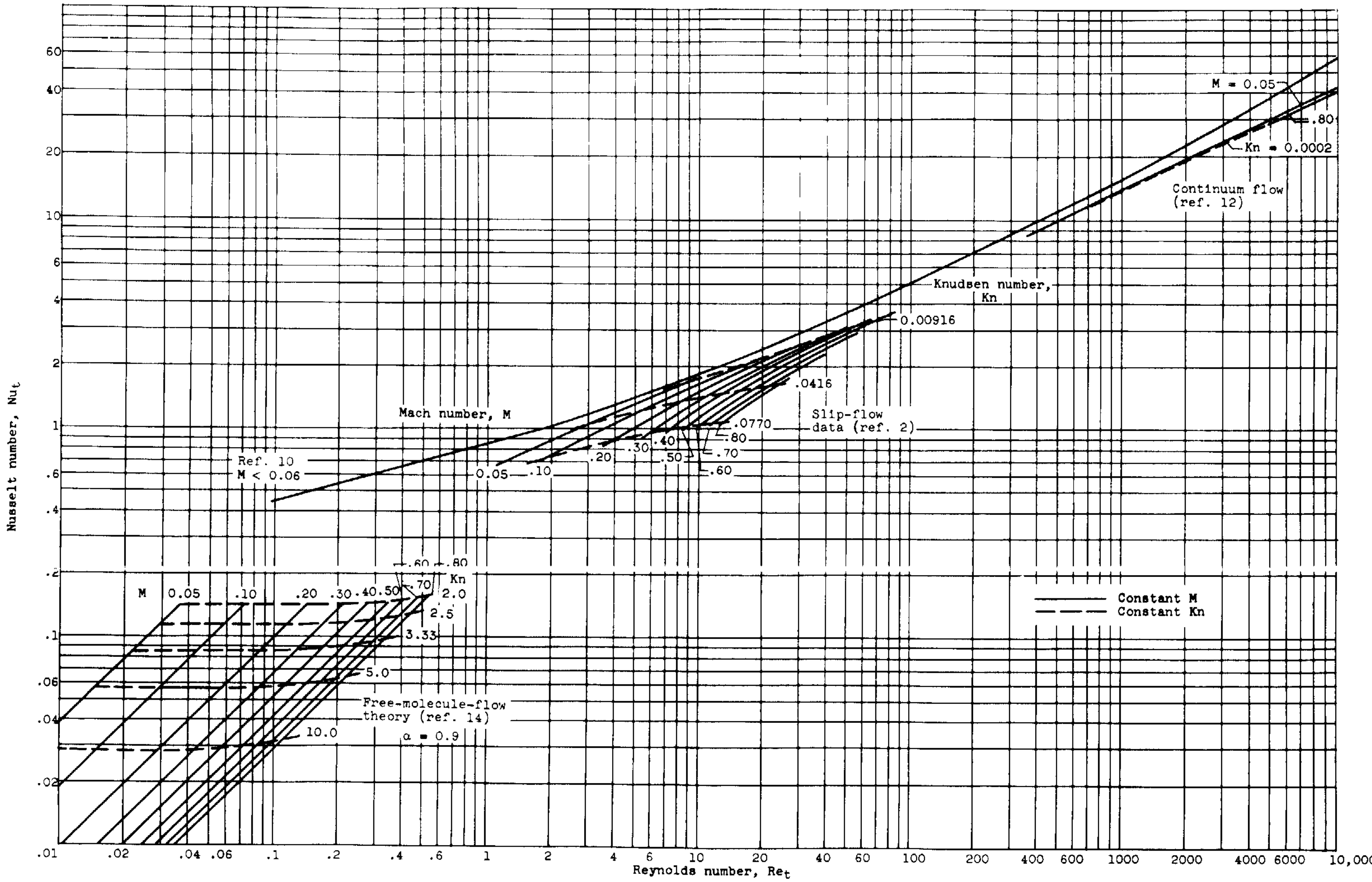

Figure 10. - Attempted Nusselt number correlation for cylinders in subsonic continuum, slip, and free-molecule flows.

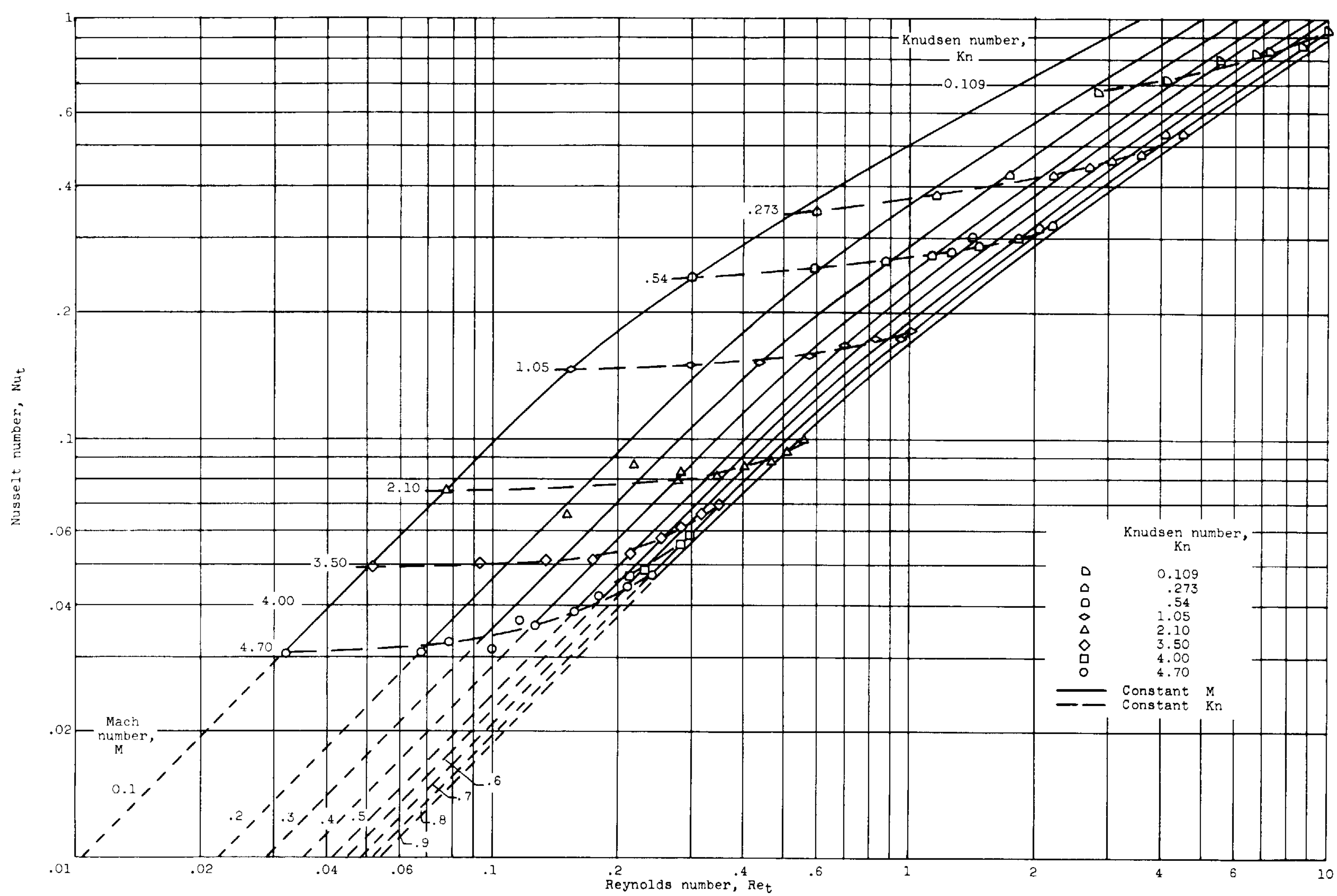

Figure 11. - Nusselt number correlation for cylinders in subsonic flow. Total air temperature, 80° F; length-average wire temperature, 580° F.

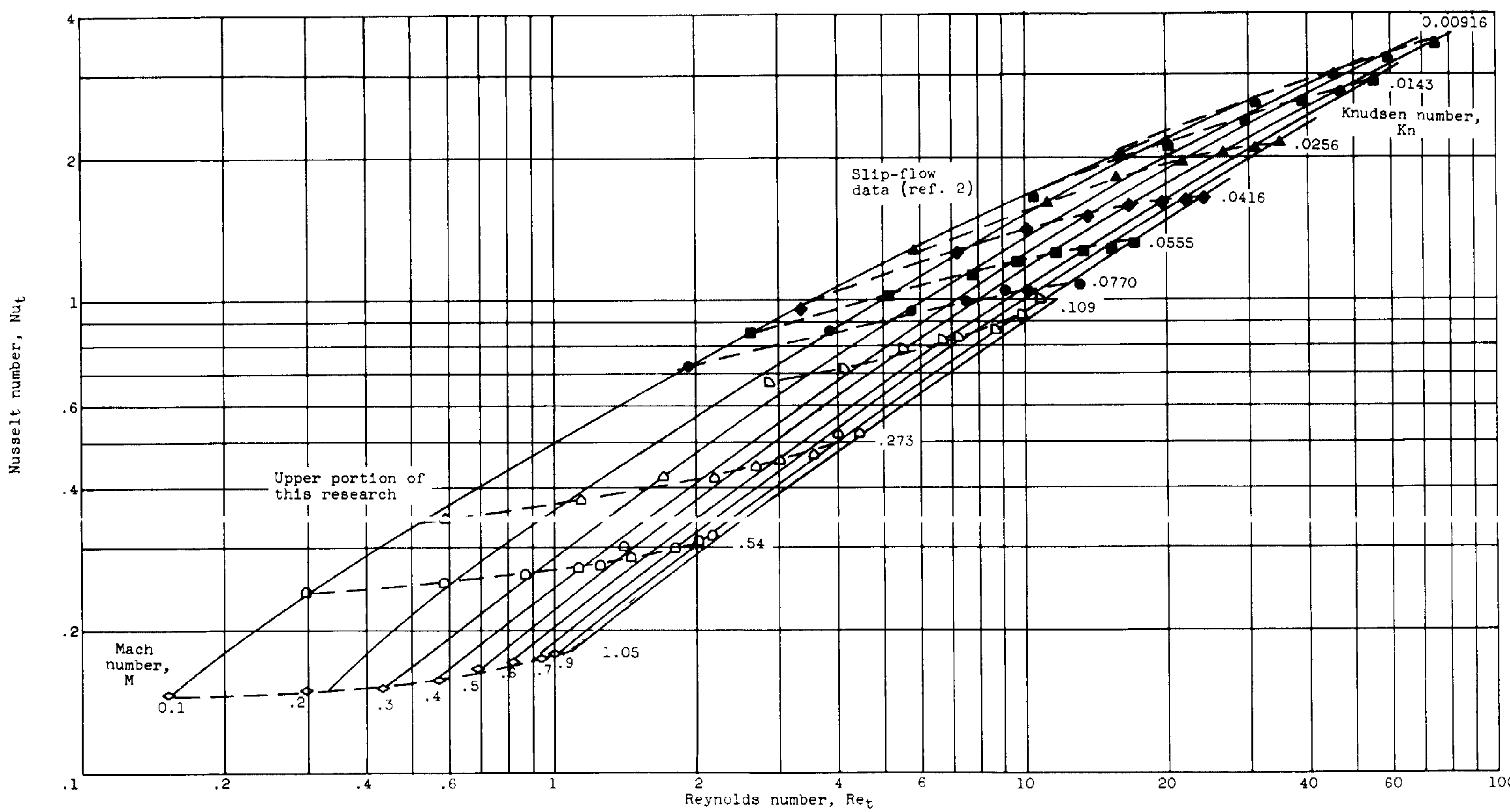

Figure 12. - Comparison of heat-transfer data with previous slip-flow data.

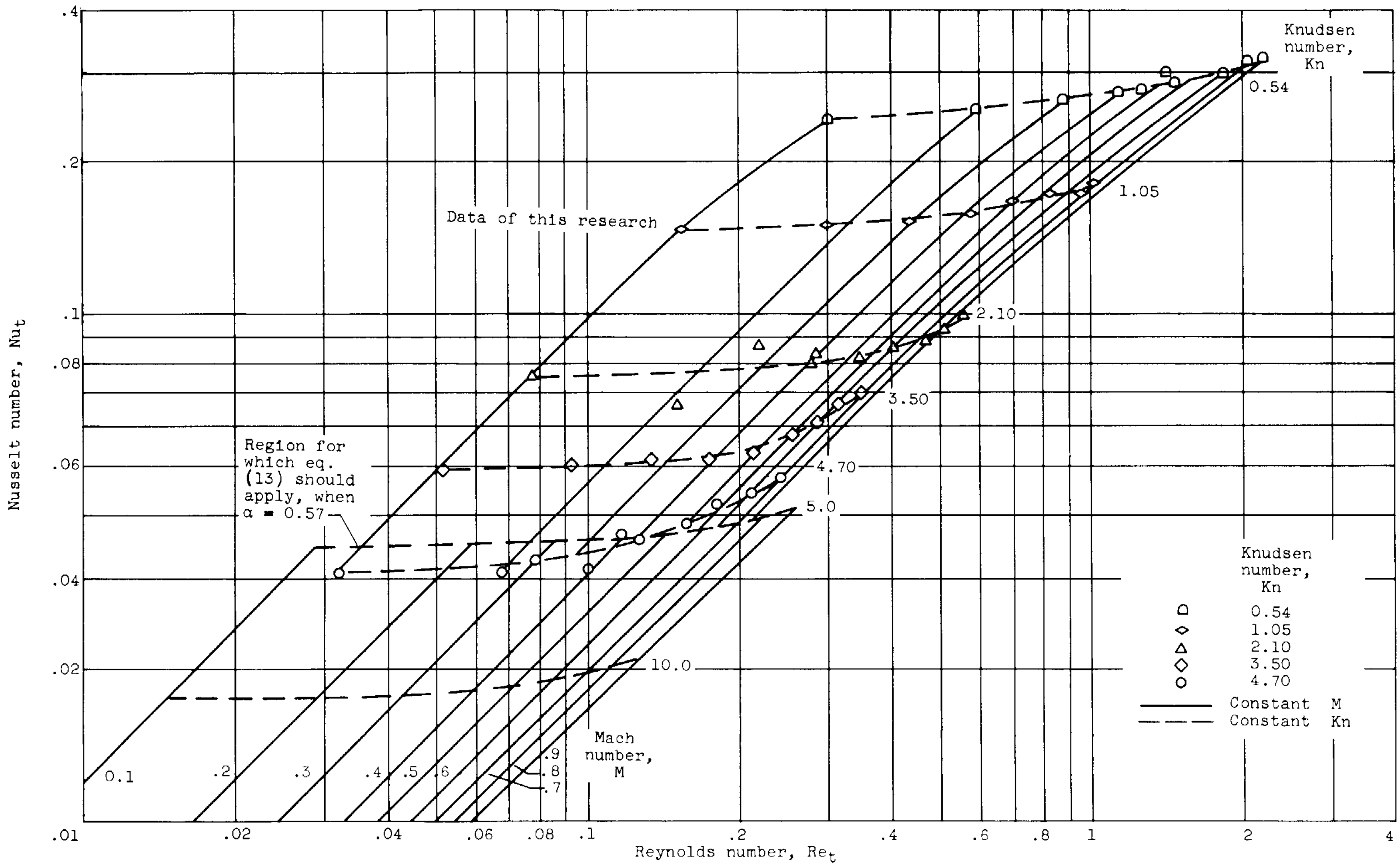

Figure 13. - Comparison of heat-transfer data with free-molecule-flow theory using $\alpha = 0.57$.

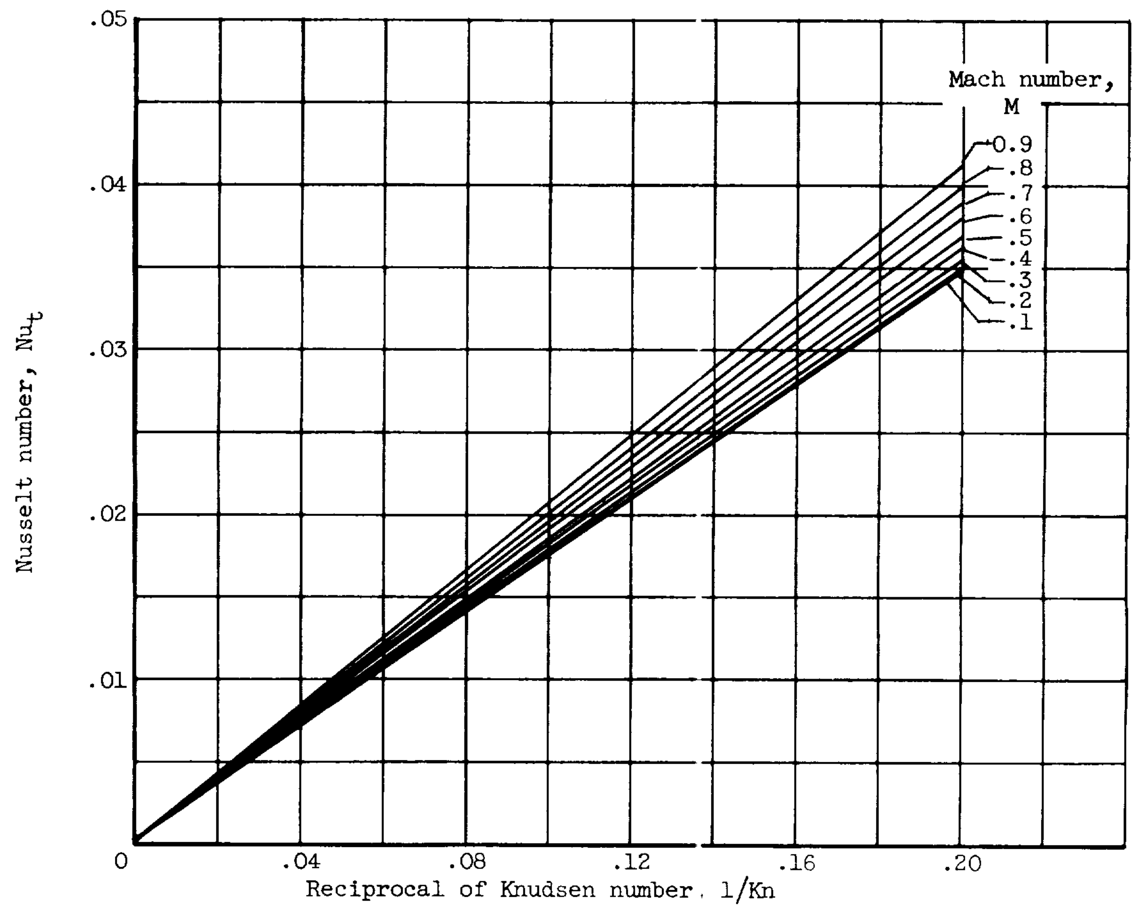

Figure 14. - Plot of equation (13) with $\alpha = 0.57$.

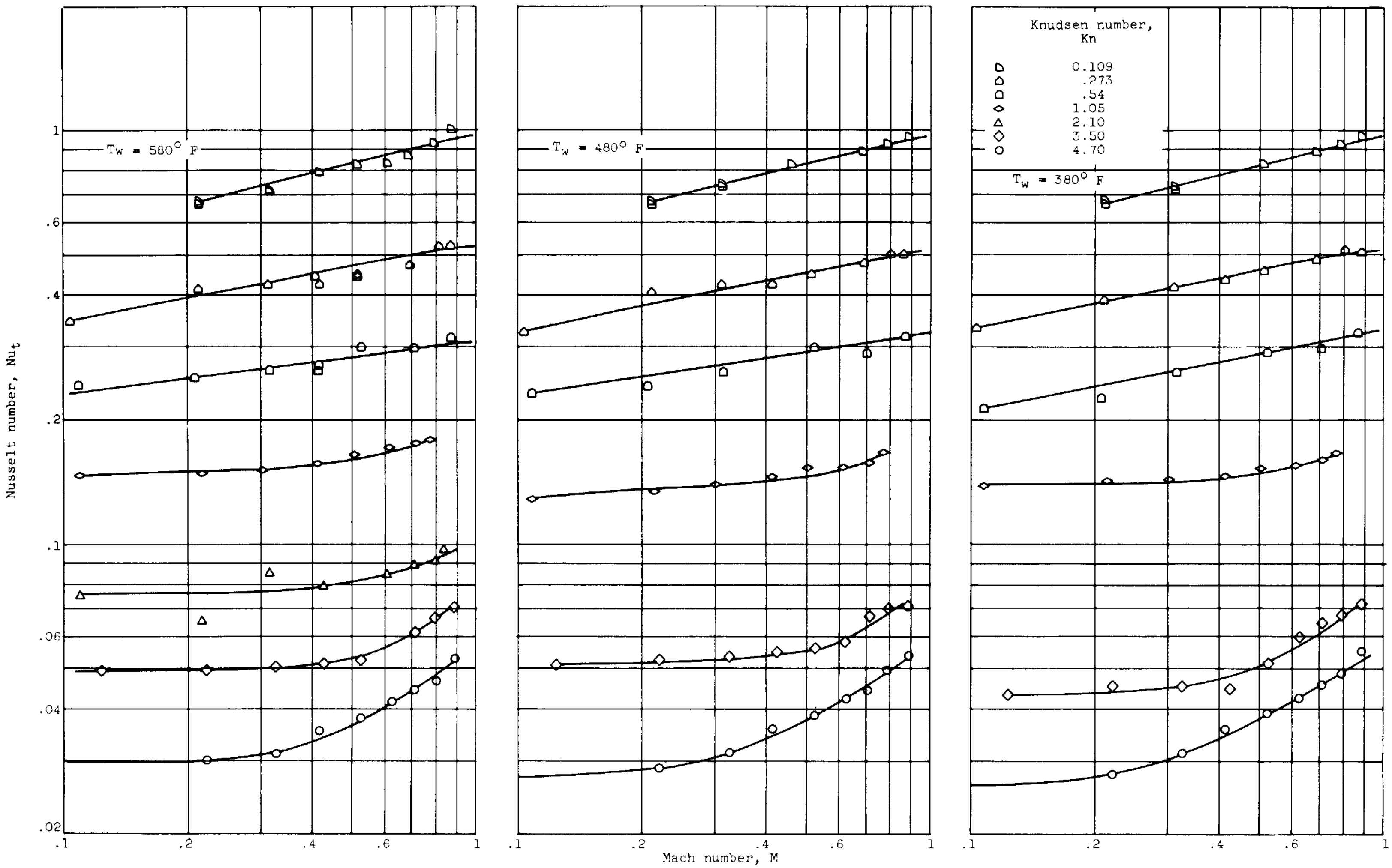

Figure 15. - Variation of Nusselt number with Mach number for constant Knudsen number and constant total air and wire temperatures. Total air temperature, 80° F.

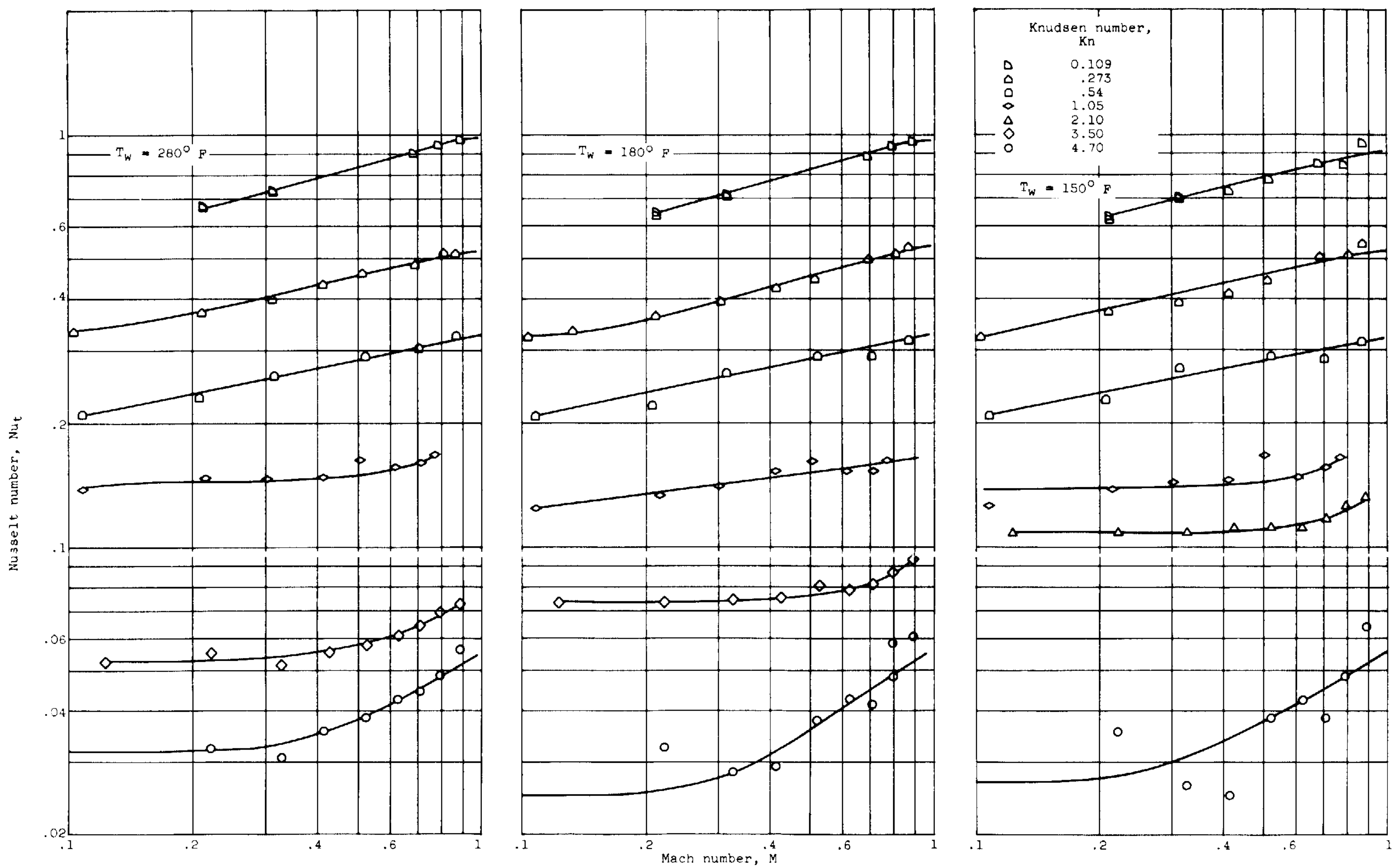

Figure 15. - Concluded. Variation of Nusselt number with Mach number for constant Knudsen number and constant total air and wire temperatures. Total air temperature, 80° F.

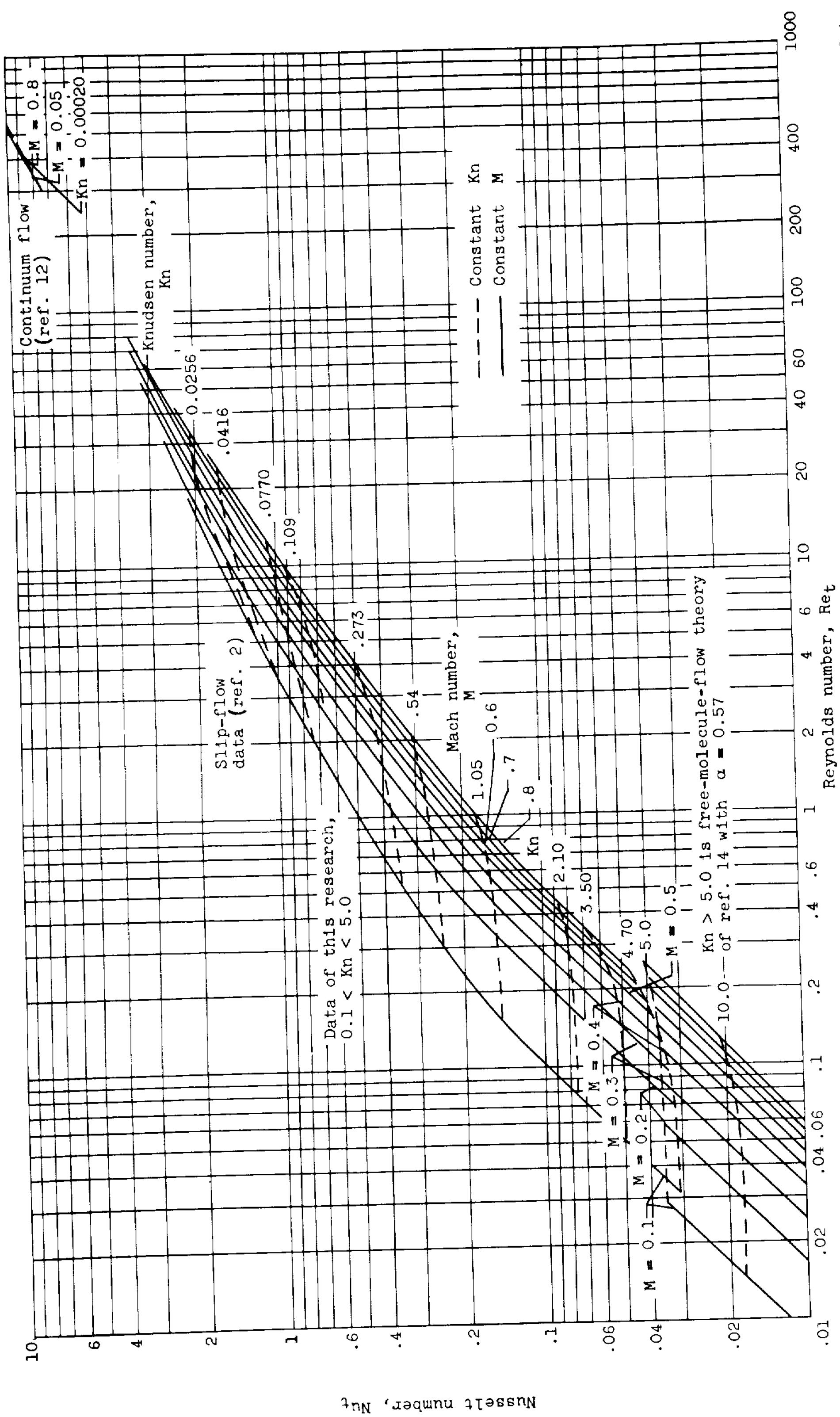

Figure 16. - Attempted Nusselt number correlation for cylinders in subsonic continuum, slip, and free-molecule flow using the data of this research and free-molecule-flow theory with $\alpha = 0.57$.